geosciences

MDPI

Review

Slab Load Controls Beneath the Alps on the Source-to-Sink Sedimentary Pathways in the Molasse Basin

Fritz Schlunegger [1,*] and Edi Kissling [2]

[1] Institute of Geological Sciences, University of Bern, 3012 Bern, Switzerland
[2] Department of Earth Sciences, ETH Zürich, 8052 Zürich, Switzerland; kissling@tomo.ig.erdw.ethz.ch
* Correspondence: fritz.schlunegger@geo.unibe.ch; Tel.: +41-31-684-8767

Abstract: The stratigraphic development of foreland basins has mainly been related to surface loading in the adjacent orogens, whereas the control of slab loads on these basins has received much less attention. This has also been the case for interpreting the relationships between the Oligocene to Micoene evolution of the European Alps and the North Alpine foreland basin or Molasse basin. In this trough, periods of rapid subsidence have generally been considered as a response to the growth of the Alpine topography, and thus to the construction of larger surface loads. However, such views conflict with observations where the surface growth in the Alps has been partly decoupled from the subsidence history in the basin. In addition, surface loads alone are not capable of explaining the contrasts in the stratigraphic development particularly between its central and eastern portions. Here, we present an alternative view on the evolution of the Molasse basin. We focus on the time interval between c. 30 and 15 Ma and relate the basin-scale development of this trough to the subduction processes, and thus to the development of slab loads beneath the European Alps. At 30 Ma, the western and central portions of this basin experienced a change from deep marine underfilled (Flysch stage) to overfilled terrestrial conditions (Molasse stage). During this time, however, a deep marine Flysch-type environment prevailed in the eastern part of the basin. This was also the final sedimentary sink as sediment was routed along the topographic axis from the western/central to the eastern part of this trough. We interpret the change from basin underfill to overfill in the western and central basin as a response to oceanic lithosphere slab-breakoff beneath the Central and Western Alps. This is considered to have resulted in a growth of the Alpine topography in these portions of the Alps, an increase in surface erosion and an augmentation in sediment supply to the basin, and thus in the observed change from basin underfill to overfill. In the eastern part of the basin, however, underfilled Flysch-type conditions prevailed until 20 Ma, and subsidence rates were higher than in the western and central parts. We interpret that high subsidence rates in the eastern Molasse occurred in response to slab loads beneath the Eastern Alps, where the subducted oceanic slab remained attached to the European plate and downwarped the plate in the East. Accordingly, in the central and western parts, the growth of the Alpine topography, the increase in sediment flux and the change from basin underfill to overfill most likely reflect the response to slab delamination beneath the Central Alps. In contrast, in the eastern part, the possibly subdued topography in the Eastern Alps, the low sediment flux and the maintenance of a deep marine Flysch-type basin records a situation where the oceanic slab was still attached to the European plate. The situation changed at 20 Ma, when the eastern part of the basin chronicled a change from deep marine (underfilled) to shallow marine and then terrestrial (overfilled conditions). During the same time, subsidence rates in the eastern basin decreased, deformation at the Alpine front came to a halt and sediment supply to the basin increased possibly in response to a growth of the topography in the Eastern Alps. This was also the time when the sediment routing in the basin axis changed from an east-directed sediment dispersal prior to 20 Ma, to a west-oriented sediment transport thereafter and thus to the opposite direction. We relate these changes to the occurrence of oceanic slab breakoff beneath the Eastern Alps, which most likely resulted in a rebound of the plate, a growth of the topography in the Eastern Alps and a larger sediment flux to the eastern portion of the basin. Beneath the Central and Western Alps, however, the continental lithosphere slab remained attached to the European plate, thereby resulting in a continued downwarping of the plate in its central and western portions. This plate downwarping

check for updates

Citation: Schlunegger, F.; Kissling, E. Slab Load Controls Beneath the Alps on the Source-to-Sink Sedimentary Pathways in the Molasse Basin. *Geosciences* **2022**, *12*, 226. https://doi.org/10.3390/geosciences12060226

Academic Editors: Olivier Lacombe and Jesus Martinez-Frias

Received: 23 February 2022
Accepted: 24 May 2022
Published: 27 May 2022

Publisher's Note: MDPI stays neutral with regard to jurisdictional claims in published maps and institutional affiliations.

Copyright: © 2022 by the authors. Licensee MDPI, Basel, Switzerland. This article is an open access article distributed under the terms and conditions of the Creative Commons Attribution (CC BY) license (https://creativecommons.org/licenses/by/4.0/).

source: https://doi.org/10.48350/170338 | downloaded: 26.4.2024

beneath the central and western Molasse together with the rebound of the foreland plate in the East possibly explains the inversion of the drainage direction. We thus propose that slab loads beneath the Alps were presumably the most important drivers for the development of the Molasse basin at the basin scale.

Keywords: Molasse basin; Alps; foreland basin evolution; subduction tectonics

1. Introduction

A foreland basin is a flexural trough adjacent to an orogen where slab loads and subduction tectonics cause a flexural downwarping of the plate and the formation of a sedimentary basin, and where orogenic processes result in the creation of surface loads [1]. Because of the link between these processes, the source-to-sink routing of clastic material and the resulting stratigraphic architectures of foreland basins are considered to depend on the tectonic development in the adjacent orogen [2–5]. This perception is based on the results of numerical models [6–8], which use the concept of an elastic plate overlying a fluid substratum such as the mantle [9]. Such models were applied for the first time in the early 80's by the pioneering contributions by T. Jordan [10] and C. Beaumont [11] who calculated the deflection of an elastic plate [10], or a foreland plate with a visco-elastic rheology [11] to applied loads. Such models, and particularly approaches that are based on a fully elastic rheology, predict that the basin width depends on the elastic strength of the foreland plate, whereas the basin depth hinges on both the plate's strength and the loads [9]. Among the potential loads (Figure 1), most attention has been focused on relating the basin architecture to the evolution of surface loads in the orogen, mainly because it was recognized from early onward that foreland basins contain the erosional products of the adjacent orogen [12], and as such, should contain information on how the mountain belt topography evolved through time. The focus on the surface topography, and thus on the surface loads, resulted in a view where changes in the basin's development were caused by thrusting along individual faults or in a spatially limited area [6–8]. This is particularly the case for the Molasse foreland basin situated on the northern side of the European Alps [6,13–17]. This basin, which extends from Chambery to Linz over an along-strike distance of c. 850 km and which has a maximum cross-sectional width of c. 150 km (Figure 2), has evolved in response to the Alpine orogeny since the Late Cretaceous and records early underfilled (Flysch stage) and subsequently filled to overfilled conditions (Molasse stage) [18]. Numerous chronologic, stratigraphic, sedimentologic and provenance tracing analyses have resulted in a level of detail that is probably one of the highest for a foreland basin [12–17,19–24]. In this context, reconstructions of how the surface loads in the Alps evolved through space and time have been the preferred focus, if the aim was to use stratigraphic data from the Molasse basin to reconstruct Alpine orogenic events. Among such efforts, Pffifner's work [13] was the first contribution which related the subsidence history of the Swiss part of the Molasse basin to the history of thrusting and loading in the upper crust, and thus to the buildup of topographic loads in the frontal part of the Alps. Other authors followed the same scope, but they applied theoretical models that were based on the principle where an elastic plate overlies a fluid substratum such as the mantle [9]. Recently, the views where topographic loads alone explain the continuous subsidence of the Molasse basin have been contested [25,26], mainly because of lack of evidence for a contemporaneous growth of the topography at the scale of the Central Alps [26,27]. However, possible controls of subduction tectonics on the stratigraphic development at the basin scale and the routing of the clastic detritus to the sedimentary sink have been largely unexplored [28]. This is mainly the case because of the lack of required information such as patterns of slab loads beneath the Alps being unavailable until 2003 when high-resolution seismic tomography images became available for the first time [29].

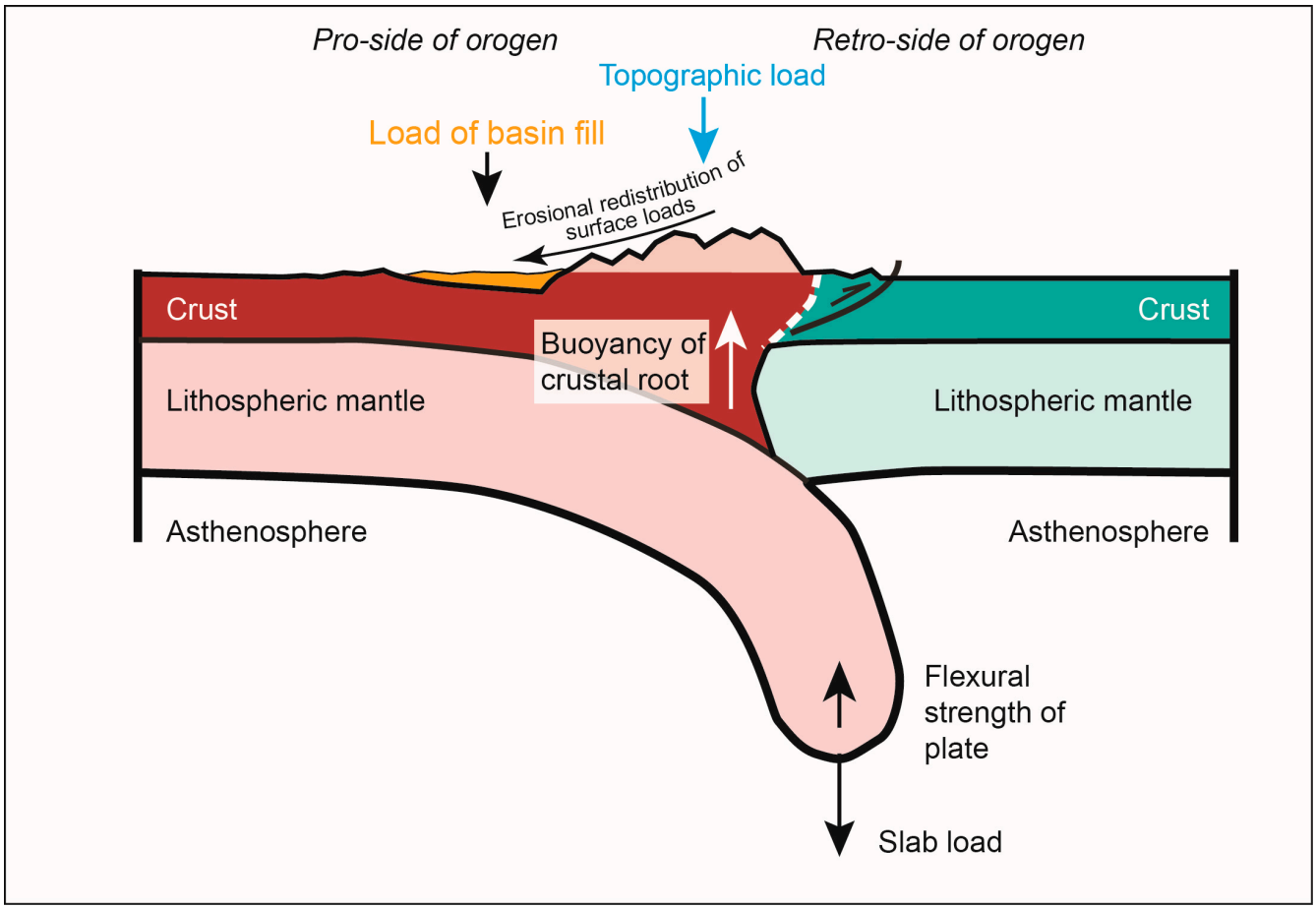

Figure 1. Orogenic and basin loads and flexure of a foreland plate. Modified from Schlunegger and Kissling [26].

Here, we focus our work on the European Alps and the Molasse foreland basin (Figure 2), and we relate the evolution of the stratigraphic record preserved in this basin to the large-scale tectonic development of the Alpine orogen. We particularly elaborate how the combination of European lithosphere slab and topography loads exert a downward-directed force on the foreland plate, and how they controlled together with the buoyancy of an evolving crustal root the geodynamic development of the Alpine orogen (Figure 1). The combined effects of these forces are mirrored by the generation of sediment in the mountain belt through erosion, by the routing of this material to the foreland trough and by the preservation of the resulting signals in the stratigraphic record. This work is thus mainly based on a compilation of tectonic data from the Alps and stratigraphic data from the Molasse basin in an effort to relate the subduction tectonics that shaped the Alps to the development of the Molasse basin situated on the northern side of this orogen.

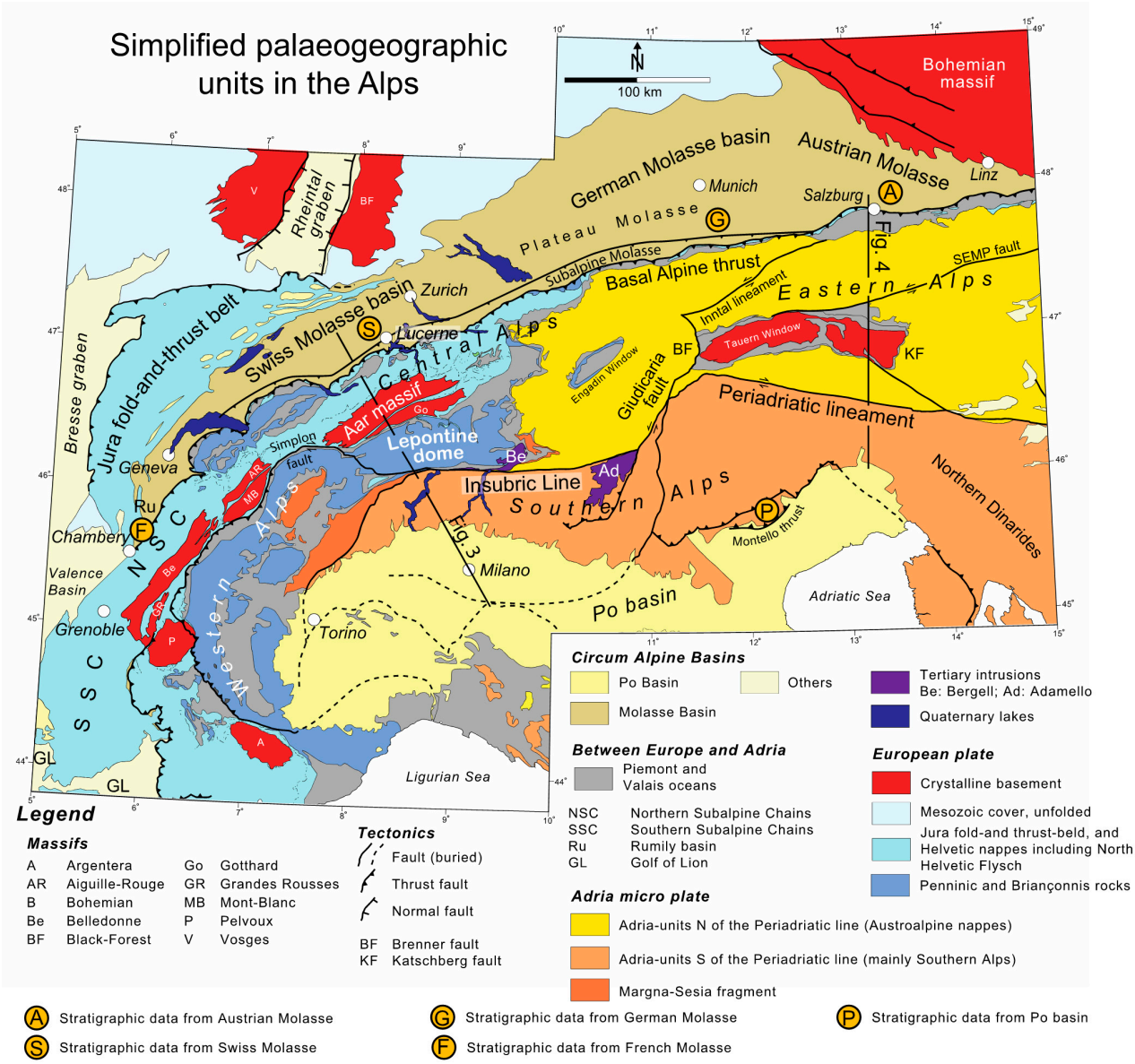

Figure 2. Geological map of the Western, Central, Eastern and Southern European Alps [30–33]. Rocks of European origin occur in the Jura fold-and-thrust belt, in the Northern (NSC) and Southern Subalpine Chains (SSC), and along the thrust front of the Central and Eastern Alps (Helvetic nappes). Slivers of the Iberian plate (e.g., Briançonnais rocks and crystalline basement rocks in the hangingwall of the Simplon fault) were part of the European plate since c. 35 Ma. The Lepontine dome is a structure that was exhumed through slip along the Simplon fault. It exposes high-grade basement rocks of European origin. The lithologies of the Adriatic continental plate constitute the Southern and Eastern Alps and cover a large area. During the Mesozoic phase of spreading, the continental plates were separated by the Valais and Piemont Oceans. The related (meta)sedimentary rocks were thrust on top of units of European origin during the Alpine orogeny. A major tectonic fault, referred to as the Periadriatic lineament (or Insubric Line west of the Giudicaria fault), separates the northern from the southern portions of the Alps with north- and south-vergent thrusts, respectively. Backthrusting along this fault facilitated the rise of the Tertiary magmas. This fault was offset by left-lateral faulting along the Giudicaria fault. The Alps are bordered by the Molasse foreland basin in the North and the Po basin in the South: A (Austrian Molasse), G (German Molasse), S (Swiss Molasse), F (French Molasse) and P (Po basin) are the sites for which stratigraphic data was used to reconstruct the subsidence history of the foreland plate.

2. Geological Setting

2.1. Crustal-Scale Architecture of the Alps

The current litho-tectonic architecture of the European Alps (Figure 2) is the result of the collision between the European plate, slivers of the Iberian plate and the Adriatic continental plate in the West, and the European and Adriatic plates in the East [31–37]. Subduction of the European plate started in the Late Cretaceous [34]. It resulted in the closure of the Valais Ocean between the European and Iberian plates and of the Piemont Ocean separating the Adriatic and the European plates [32,34]. Both oceans were originally formed in response to the Mesozoic phase of spreading. Subduction finally culminated in the continent-continent collision between these plates and in the construction of the Alpine orogen [34]. On the northern and western margin of the Alps, the orogen comprises low-grade to non-metamorphosed rocks derived from the European continental plate and its stretched margin during Mesozoic times. These rocks are exposed in the Jura fold-and-thrust belt in the Central Alps, the Helvetic thrust nappes in the Central and Eastern Alps, and in the Northern and Southern Subalpine Chains in the Western Alps (NSC and SSC; Figure 2). In the central part of the orogen, uplifted crystalline blocks together with their autochthonous sedimentary cover that are also derived from the European continental plate are exposed in the external massifs [38] (e.g., the Belledonne massif in the Western Alps, the Aar massif in the Central Alps, and the Tauern Window in the Eastern Alps; Figure 2). These units are overlain by the Penninic thrust nappes that were partly derived from the Iberian plate. They occur as sedimentary thrust sheets in the northern margin of the Western and Central Alps (Briançonnais unit), or as medium- to high-grade crystalline rocks in the Lepontine Dome (Figure 2). On the eastern and southern sides of the Alps, the north-vergent Eastern and south-vergent Southern Alps are mainly made up of rocks derived from the Adriatic continental plate, and lithologies of the Iberian plate are absent. The northern and southern parts of the Alps are separated by the Periadriatic lineament (or Insubric Line west of the Giudicaria fault), which accommodated the Late Oligocene to Early Miocene shortening by backthrusting and right lateral slip [34]. This fault also offered the pathways for the Tertiary intrusions [34]. The Insubric Line/Periadriatic lineament was offset through left lateral faulting along the Giudicaria fault, which occurred in response to the post-20-Ma old shortening of the Southern Alps [39–41]. Finally, the Eastern Alps are characterized by several left-lateral faults (such as the Inntal lineament and the SEMP fault, Figure 2) that have dissected the orogen leading to large-scale lateral extrusion since c. 20 Ma [40,42,43].

Published tectonic cross sections that are based on geological maps [30–33] and seismic surveys in combination with seismic tomography investigations [29,44] allowed to extend the surface geology to greater depths and to develop a simplified geological-geophysical model of the Alps (Figure 3). Accordingly, beneath the Central Alps, a c. 160 km-long lithospheric mantle slab that is part of the European continental plate dips towards the South and exerts a downward-directed slab load force (Figure 3B). This load together with surface topography loads are counterbalanced by the buoyancy of the crustal root extending to more than 50 km depth [34]. The root comprises a stack of lower crustal material that was accreted, most likely from the extended European margin and the Iberian plate, during the Paleocene to Miocene [45]. The occurrence of a buoyant crustal root was also used to explain the negative Bouguer anomaly in the area surrounding the Central Alps [46,47]. Beneath the Western Alps, a tear appears to separate the subducted slab from the European plate [29,33], which has been contested [48]. However, we consider the interpretation of a still attached slab beneath the Western Alps as biased because it is based on seismic data where the signal to noise ratio is lower than in Lippitsch and co-authors [29]. Furthermore, the interpretation where the slab is still attached to the European plate was recently challenged documenting a detached slab [49]. Therefore, we consider the interpretation by Lippitsch and co-authors [29] of a detached slab as more convincing than the view in [48] where the European lithospheric mantle slab is still attached to the European plate.

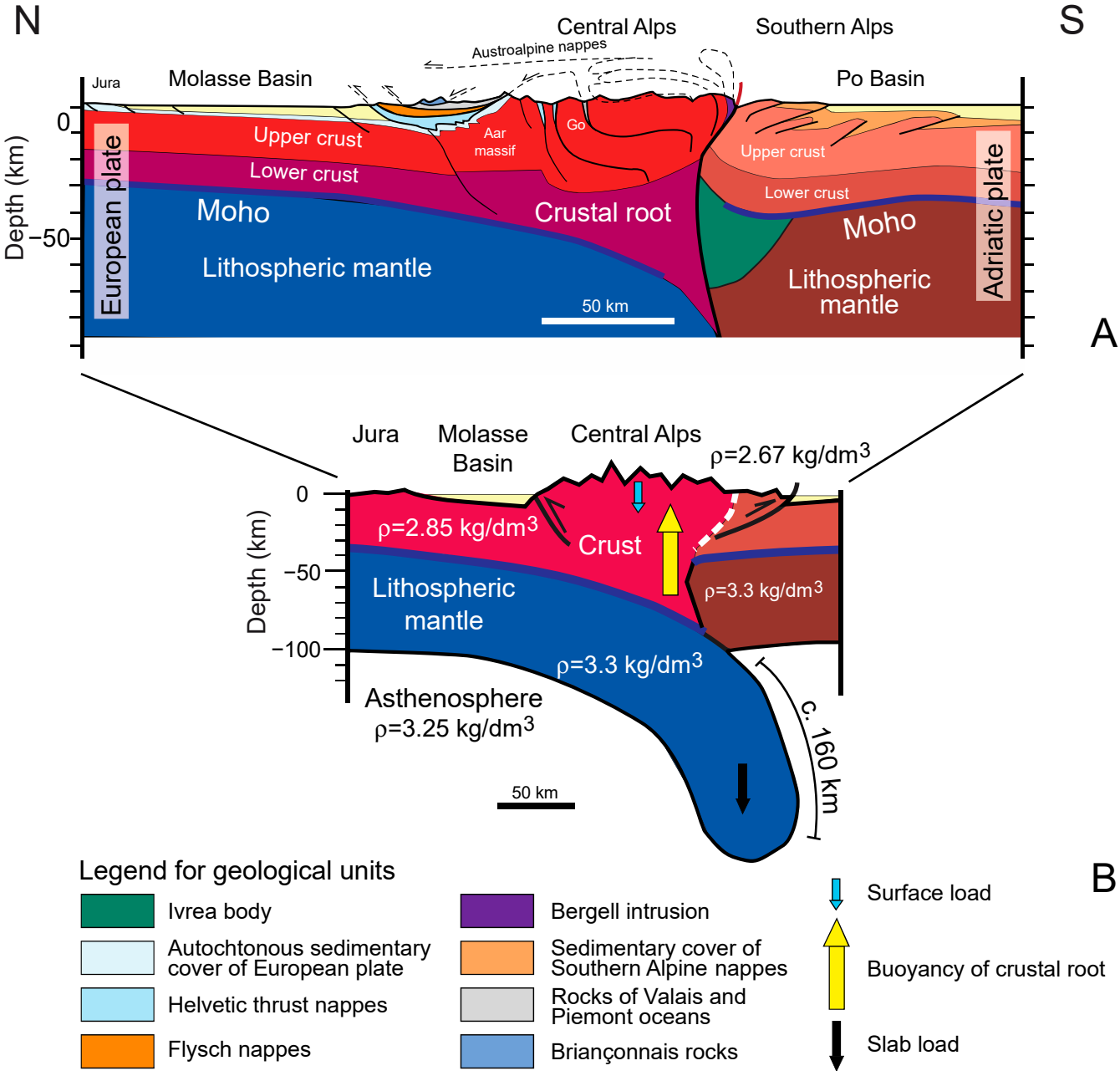

Figure 3. (**A**) Tectonic section across the Central Alps [33] (for location see Figure 2). On the northern side, the orogen comprises a nappe stack derived from the European plate and its stretched margin together with slivers of the Iberian plate that formed part of the European plate since 35 Ma. (**B**) Simplified geological-geophysical model of the Central Alps (along same section as Figure 3A), derived from seismo-tomographic images [29,33]. The lithospheric mantle has a greater density than the asthenosphere. Therefore, it exerts a downward-directed slab load force. The crustal root, occurring at deep levels, comprises lower crustal rocks, which were derived through accretion of material from the Iberian plate and the European margin. These rocks have a lower density than the asthenosphere and thus exert a buoyancy force. The elevation of the current topography of the Central Alps thus reflects the isostatic equilibrium between these forces.

East of the Giudicaria fault (Figure 2), seismic tomography investigations disclosed the occurrence of a lithospheric slab beneath the Eastern Alps, which is c. 190 km long along the section displayed in Figure 4 [44]. Please note that along this section (Figure 4), the tectonic structures underneath the Tauern Window are poorly constrained because of a

lack of seismic data. We therefore adapted the structural style from a section through the western part of the Tauern Window where seismic data disclosed the occurrence of steep faults [50,51]. Note also that beneath the Eastern Alps, the dip of the lithospheric slab, its origin and thus its relationship to either the European or Adriatic continental plates has been controversially discussed [52]. In particular, it was proposed that this slab dips towards the NNE [29,44,53,54] and represents the subducted lithosphere mantle of the Adriatic plate [44]. Others proposed that the slab has a subvertical orientation [55,56] or might even be overturned [28], thereby representing rather a yet delaminated European lithospheric mantle slab than the continuation of an NNE-dipping Adriatic slab. However, we prefer the interpretation where the NNE dip of the high-velocity anomaly reflects the occurrence of a lithospheric mantle slab that is connected with the Adriatic plate [29,37,40,44], because it is based on the consideration of a high-resolution a priori 3D crustal model of the Alps [29,54,57,58]. In either case, the interpretation of all authors converges on the notion that the European continental plate lacks a lithospheric mantle slab beneath the Eastern Alps that is attached to the European plate and that would deflect this plate towards the South. Most authors also agree on the interpretation that this situation has prevailed since c. 20 Ma [37,40], as a balancing of the shortening in the Eastern Alps within a detailed temporal framework has shown [40]. If our preferred interpretation of an NNE-directed dip of the Adriatic lithospheric mantle slab is valid, then the boundary between the Western/Central and Eastern Alps could be placed where the change in subduction polarities occurs. According to Lippitsch et al. [29], such a change from an SE orientation underneath the Central Alps (subduction of European mantle lithosphere) to an NNE orientation underneath the Eastern Alps (subduction of Adriatic mantle lithosphere) occurs in the vicinity of the Giudicaria fault. Therefore, we place the boundary between the Western/Central and Eastern Alps along this fault [33] and its northward projection. We acknowledge that this interpretation differs from the view in which this boundary has been placed farther west where today the Austroalpine nappes start to cover the largest portion of the Alps on their northern side (Figure 2) [34]. However, excluding a change in the subduction polarity, the Giudicaria fault also separates the Alps in an eastern and a western segment. East of this fault, the post-20 Ma shortening of the South Alpine units [39,40] was accompanied by a left-lateral slip along the Giudicaria fault and by east-west extension along faults that extend from the Giudicaria fault towards the East [42,59]. In contrast, west of the Giudicaria fault, pre-20 Ma but also post-20 Ma N-S shortening was mainly accommodated by backthrusting along the Insubric Line together with some shortening in the Southern Alps. Accordingly, there is ample evidence from the deep crustal architecture and the surface geology to place the boundary between the Eastern and Western/Central Alps along the Giudicaria fault [33].

As a conclusion, if our preferred interpretation of a change of the subduction polarity at 20 Ma is valid and the interpretation of a NNE dipping Adriatic slab is appropriate, then the Molasse basin should record a signal that is different west and east of the northward continuation of the Giudicaria fault. In addition, and in contrast to the Central Alps, a thick buoyant crustal root comprising lower crustal material is largely absent beneath the core of the Eastern Alps or it is at least much thinner than in the Central Alps as suggested by the Bouguer anomaly pattern [60] and the Moho map [61] across the Alps. This explains the lower elevation of the topography in the Eastern Alps (peak altitudes of c. 3500 m a.s.l.) in comparison to the Central Alps (peak altitudes c. 4500 m.s.l.). Such a difference should be reflected in the patterns of erosion and sediment supply to the basin, which we will disclose in this work.

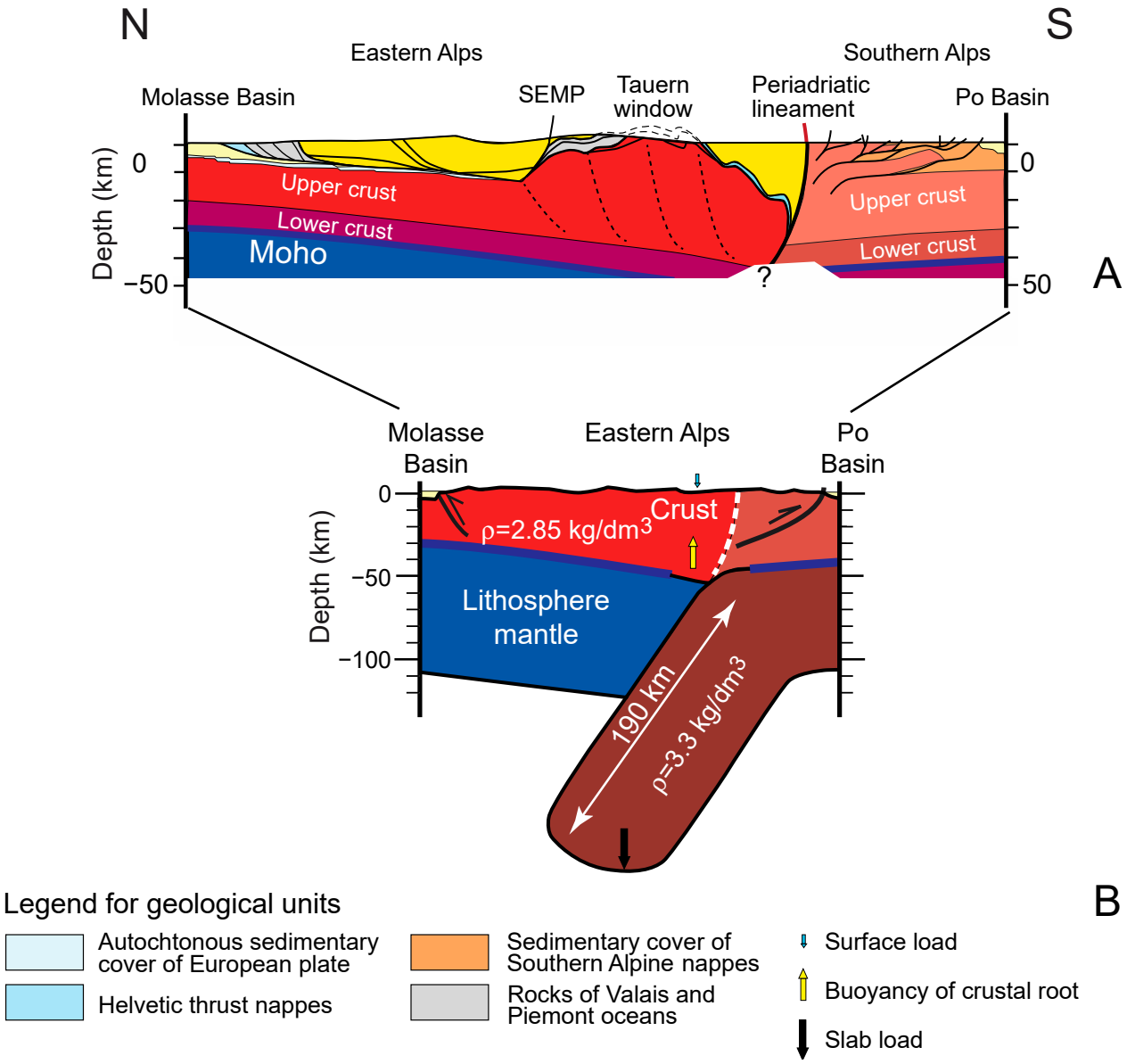

Figure 4. (**A**) Tectonic section across the Eastern Alps, modified from Rosenberg et al. [35,36] (for location see Figure 2). The cross-section shows that the orogen comprises rocks derived from the European and Adriatic continental plates, yet lithologies of Iberian origin are absent. The rocks in the Tauern Window correspond to the stretched margin of the European plate during the Mesozoic phase of spreading [31,32,35]. (**B**) Simplified geological-geophysical model of the Eastern Alps, which is derived from seismo-tomographic images [44] (along same transect as Figure 4A). Beneath the Eastern Alps, the buoyant crustal root is thinner than beneath the Central Alps, which explains the lower elevation of the surface topography in the East. This figure implies that the NNE dipping slab is of Adriatic origin [29], which has been contested [28,52]. Please refer to the text for a discussion of why we prefer the Lippitsch et al. [29] interpretation of the seismo-tomography data.

2.2. The Sedimentary Basins Surrounding the Alps

The Molasse and Po basins are the foreland sedimentary troughs situated on the northern and southern sides of the Alps, respectively. Because the Po basin sits on the Adriatic plate and since it had a position of a retro-foreland basin particularly before 20 Ma (see below for justification), the subsidence of this sedimentary trough was largely independent of the Alpine subduction-collision dynamics on a large-scale. In fact, the current very deep (>11 km) asymmetric Po foreland basin evolved as a result of the

downbending of the Adriatic lithosphere beneath the northern Apennines [62–66]. As such, it evolved in the role of a pro-foreland basin of the Apennines, but it accumulated materials mainly derived from the Alps. In case that the interpretation of a subduction polarity change beneath the Eastern Alps at c. 20 Ma [37] is valid (see Section 2.1), then the basin on the eastern side of the southern extension of the Giudicaria fault took the role as a pro-foreland basin of the Alps, in which sediment accumulation rates has increased since then. The portion of the Po basin farther west, however, has remained in a retro-foreland situation until now. As will be discussed in Section 5.3, there is evidence from the Po basin stratigraphy that supports this view.

Situated at the margin of the Molasse basin, the Bresse and Rhine graben and the Valence basin accumulated some of the Alpine material. The formation of these basins has interfered with the development of the Molasse basin at different times mainly on its distal margin and in the French part [67–69].

2.3. The Molasse Basin

The Molasse basin stretches from Chambery to Linz over an along-strike distance of c. 850 km. It has a N-S direction south of Geneva where Molasse strata occur as isolated remnants in the Southern Subalpine Chaines (SSC). East of Geneva, the basin adapts a SW-NE orientation and widens from c. 20 km to a maximum width >150 km at the latitude of Munich (Figure 2). Towards Linz, the basin narrows again to a few kilometers.

At the proximal basin border, the Molasse sediments were folded and sliced into isoclinal thrust sheets. This zone of deformed Molasse, which is referred to as the Subalpine Molasse (Figure 5, see also [70,71]), can be mapped between Chambery and Salzburg. East of Salzburg, however, no thrust sheets of the Subalpine Molasse are exposed, but folded and thrusted pre-20 Ma-old Molasse strata are overlain by flat lying post-20 Ma-old sequences, separated by an angular unconformity [72,73]. The southern margin of the Molasse basin is defined by the basal Alpine thrust that separates the Alpine nappes from the Molasse deposits (Figure 2). On the northern distal border, the Swiss part of the Molasse basin is delineated by the Jura fold-and-thrust belt, within which Molasse strata are locally preserved in synclines. Farther east, thick successions of Mesozoic limestones and marls that accumulated on the European plate and that make up the current Svabian Jura form the northern border of the Molasse basin. Towards Austria, the distal limits of the basin are demarcated by the crystalline rocks of the Bohemian massif. These basement rocks form a topographic high that is bound towards the Molasse basin by NW-SE striking Hercynian faults NW-SE [74]. Such faults possibly also controlled the eastward narrowing of the Molasse basin towards Linz (Figure 2).

The Molasse basin has a wedge-shaped cross-sectional geometry (Figure 5). The foreland plate underneath the Molasse basin dips beneath the Alpine orogen, giving way to a basin fill thickness of nearly 5 km at the Alpine border [13,35,73,75]. Whereas the amplitude of the foreland plate deflection is nearly constant along strike [35], the cross-sectional width of the basin decreases from the NE to the SW (Figure 2), with the consequence that the dip angle of the foreland plate increases in the same direction. Because surface loads (and also slab loads) mainly control the amplitude of a plate's deflection, but neither the flexural wavelength nor the curvature of the flexed plate [9], we do not consider that along-strike changes of such loads are capable of explaining the NE-SE decreasing trend of the basin width. Instead, this along-strike change in the deflection of the foreland plate could be the response to the along-strike differences of the flexural rigidity of the foreland plate where the stiffness of the plate would be higher in the NE than in the SW [76,77]. Alternatively, and possibly more likely, the foreland plate deflection could be influenced by the NE-SW trending Hercynian faults underneath the Molasse basin [74,75]. Such an interpretation is supported by results of simple flexural models. They illustrate that such inherited weaknesses in the foreland plate have the potential to localize the strain upon flexing a plate and thus to increase the deflection of the plate at the site where such weaknesses occur [78]. The faults underneath the Jura fold-and-thrust belt together

with the Hercynian faults at the southern border of the Bohemian massif could represent such weaknesses in the European foreland plate that could localize the deflection, thereby marking a distal border of the basin.

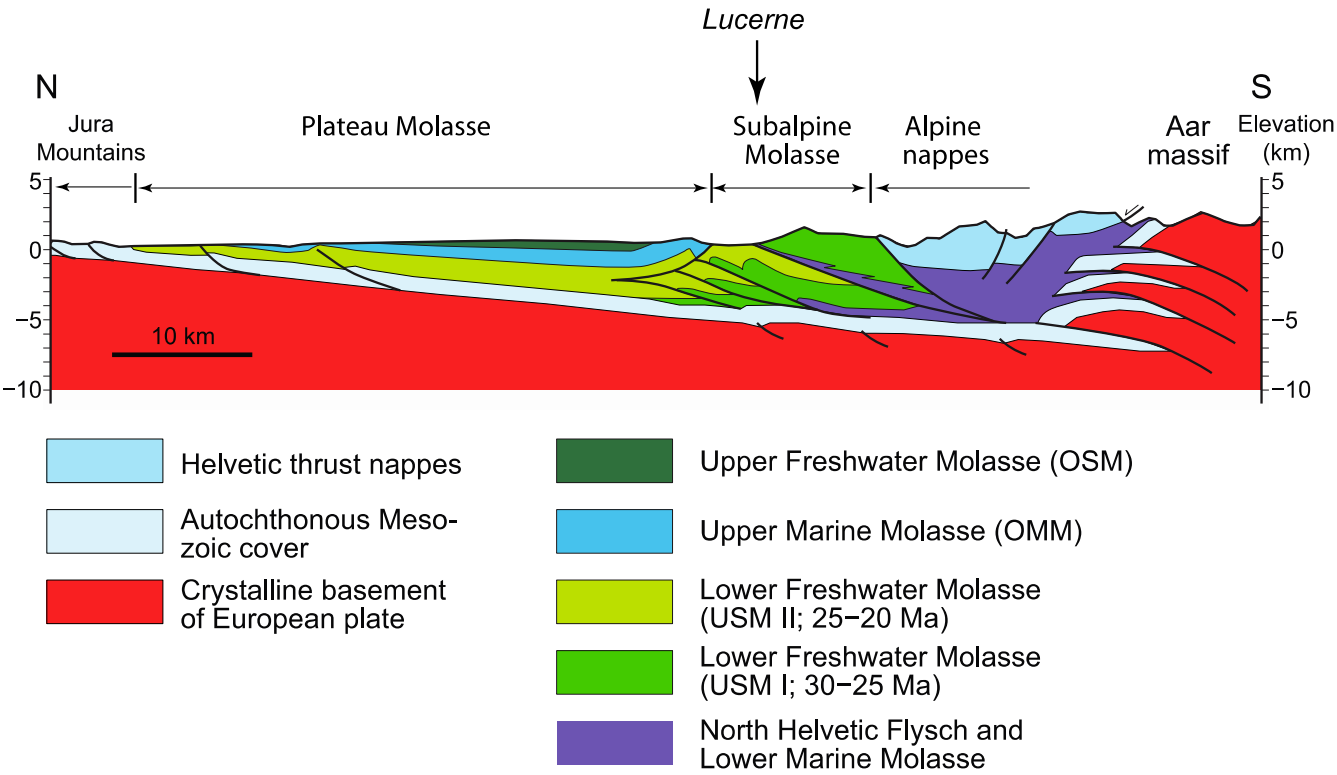

Figure 5. Tectonic section across the Swiss Molasse basin. Modified after [70,71]. The section starts in the Aar massif, crosses Lucerne and ends in the Jura fold-and-thrust belt in the North. This section runs parallel to that illustrated in Figure 3, but c. 20 km farther east. Please see Figure 2 for location of Lucerne, the Jura Mountains and the Aar massif.

The basin fill (Figure 6) consists of coarse-grained fluvial conglomerates at the proximal basin border that interfinger with finer-grained clastic material towards the basin axis. In the Swiss part of the basin, the clastic suite has generally been categorized into five lithostratigraphic groups that chronicle two shallowing and coarsening upward megasequences [79]. The first sequence starts with the North Helvetic Flysch that was deposited at c. 35 Ma. This unit then transitions into the regressive sequence of the Lower Marine Molasse group, the deposition of which gave way to the terrestrial Lower Freswhater Molasse group at c. 30 Ma according to magneto-polarity stratigraphies [14,16]. Accordingly, 30 Ma was the time when the underfilled Flysch stage evolved to the filled/overfilled Molasse stage [18]. Fluvial conditions prevailed until 20 Ma. At that time, a transgression marked the start of the second megasequence, which started with the shallow marine Upper Marine Molasse Group and ended, at c. 16.5 Ma, with the accumulation of the terrestrial Upper Freshwater Molasse group. These ages were established with magneto-polarity chronologies that were combined with mammal biostratigraphy [14,16,17].

In the Austrian part of the Molasse basin, however, the transition from deep to shallow marine and terrestrial conditions [19], and thus from the underfilled Flysch stage to the overfilled Molasse stage of foreland basin development occurred at 20 Ma [19], and thus 10 Ma later than in the Swiss part of the Molasse basin. Ages for this transition were established based on a combination of foraminiferal assemblages, coccoliths and chemostratigraphy [19]. Interestingly, the transition between the Austrian the Swiss portions of Molasse basin evolution occurred in the northern continuation of the Giudicaria fault, and thus in the vicinity of Munich. There, between 30 and 20 Ma, the shallow marine

deposits of the Chattian Sands and of the Nantesbuch Sandstone (Figure 6) recorded a transition from the terrestrial and thus the overfilled western part of the Molasse basin to the underfilled Flysch trough farther east [80]. Note that in the Munich area, the assignments of lithostratigraphic units and the chronological framework are based on correlations of resistivity and SP (spontaneous potential) logs between drillings and stratigraphic analyses of seismic sections [81,82]. Therefore, the age assignments must be considered with caution. Nevertheless, despite potential uncertainties, the results will not change the overall picture where, between c. 30 and 20 Ma, the facies transitioned from a shallow marine environment into a deep Flysch basin along strike from Munich to Salzburg [19].

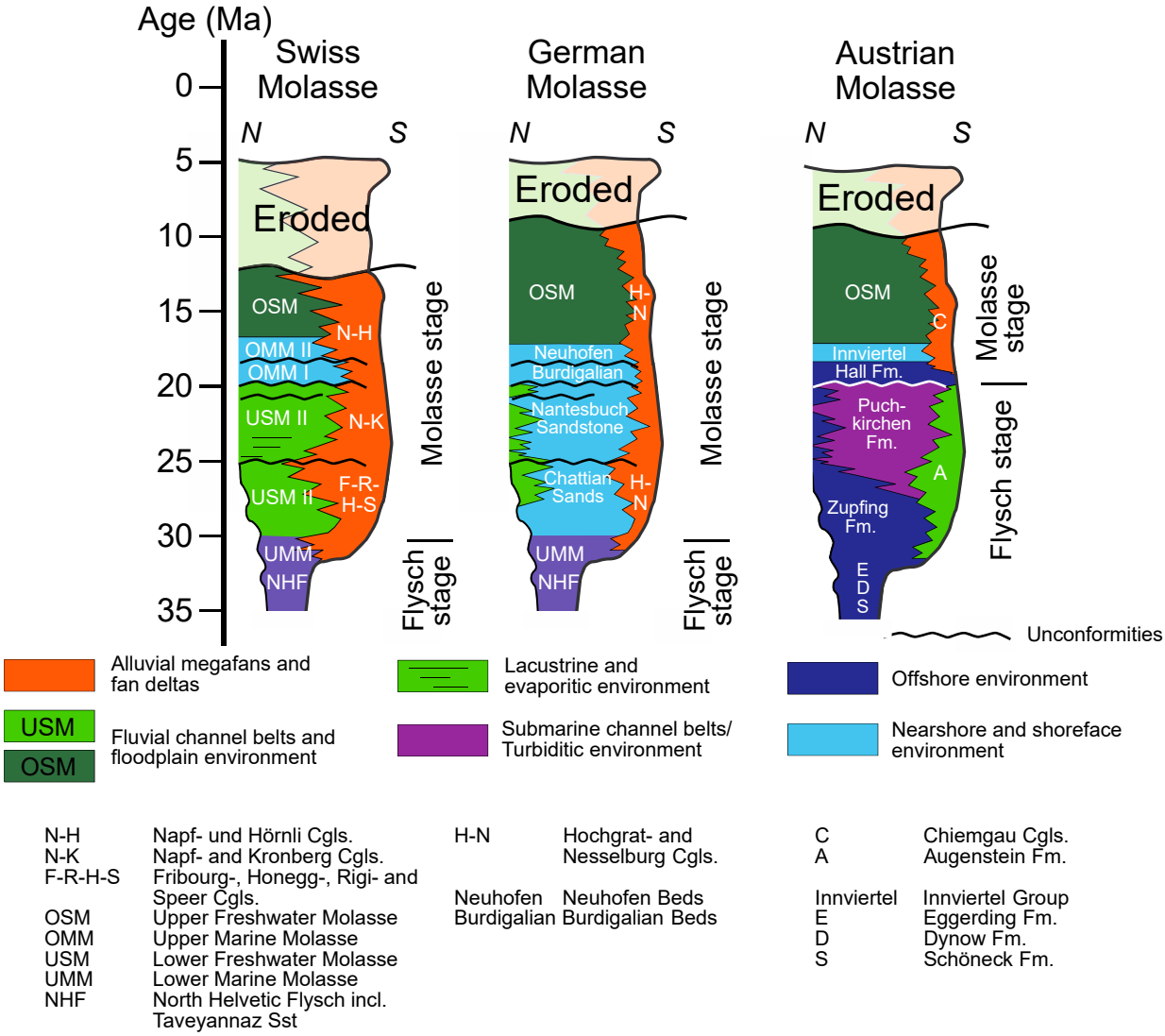

Figure 6. Stratigraphic architectures for the Swiss Molasse basin (between Geneva and Zürich), the German Molasse basin near Munich c. 20 km west of the northward extension of the Giudicaria fault, and the Austrian part of the Molasse basin between Salzburg and Linz (Figure 2). Coarse-grained alluvial megafans and fan deltas established at the Alpine thrust front. Whereas the transition between the Flysch to the Molasse stages occurred at c. 30 Ma in the Swiss Molasse, the same change in basin evolution occurred 10 Ma later in the Austrian part of the basin. Obviously, the strata near Munich chronicle the along-strike transition between the Swiss and Austrian Molasse basin. Interestingly, this is also the region that is situated in the northward extension of the Giudicaria fault where the polarity of the subducted lithospheric mantle slabs is considered to change from an SE to an NNE orientation [29].

In the entire basin, Molasse sedimentation continued up to c. 10–5 Ma [71,83–85], when a large-scale phase of uplift inverted the basin, giving way to period of erosion and erosional recycling of the foreland basin deposits, which is still ongoing. Here, a chronological assignment of basin inversion is based on apatite fission track ages that were established on sedimentary material collected from deep drillings in the Swiss Molasse basin. Using such data, Cederbom et al. [71,83] could identify the depth of the fossiliferous annealing zones in the drillings, which are situated at shallower levels than the modern fission track annealing zones. These depth differences allowed Cederbom et al. [71,83] to estimate the amount of uplift and erosion. In addition, the fission track ages recorded in the fossiliferous annealing zone were used by the same authors to determine an age when the inversion started.

3. Datasets and Methods

3.1. Sequential Restoration of the Shortening of the Alpine Orogen

For the Central Alps (Figure 3), the timing of shortening and the sequential restoration of the Central Alps have been modified from a previous publication [33]. Between 32 and 30 Ma, however, the amount of subduction and the length at which the Adriatic plate shifted towards the North is not well constrained. In our restoration, we considered that the orogenic lid did not experience much shortening during this time span. For line-balancing purposes, we therefore inferred that the length Δ_1 (Figure 7A,B) at which the northern Alpine front propagated northward corresponds to the northward shift of the Adriatic continental plate. For the subsequent collisional history of the Central Alps until the present, illustrated in the simplified Figure 7C–E, we considered that the subduction depth of the European mantle slab (c. 160 km, Δ_2) [29] was equivalent to the northward shift of the Adriatic plate [26].

For the Eastern Alps (Figure 4), we used the tectonic cross-section from Rosenberg and co-authors [35] and a simplified geological-geophysical model (Figure 4B) as a basis. For this section, the depth of the Moho is based on seismic tomography data [61,86]. The timing of the inferred subduction reversal is mainly based on the results of line- and mass-balanced structural restorations, which show that the post-20 Ma movement of the Adriatic plate together with its anticlockwise rotation resulted in a 190 km northward shift of this plate (Δ_3, Figure 7J) where we placed our section through the Eastern Alps [40]. This northward displacement corresponds to the length of the subducted mantle slab beneath the Eastern Alps [44]. These movements resulted in a dissection and a c. 70 km (our estimate) to 80 km (in Linzer et al. [59]) northward displacement of the Periadriatic lineament (Δ_4, Figure 7J), which was accomplished by left-lateral faulting along the Giudicaria fault [40]. Note that because of the syntectonic emplacement of 32 Ma-old tonalitic intrusions along the Giudicaria fault, NE-SW faulting along this fault was also considered to have started earlier. However, it is very likely that the tonalitic intrusion occurred simultaneously with E-W faulting along the Periadriatic lineament, and that the batholits were subsequently rotated into the Giudicaria fault system (see discussion and references in Rosenberg et al. [36]). Nevertheless, the occurrence of some pre-20 Ma-displacement along this fault is possible but cannot be precisely quantified.

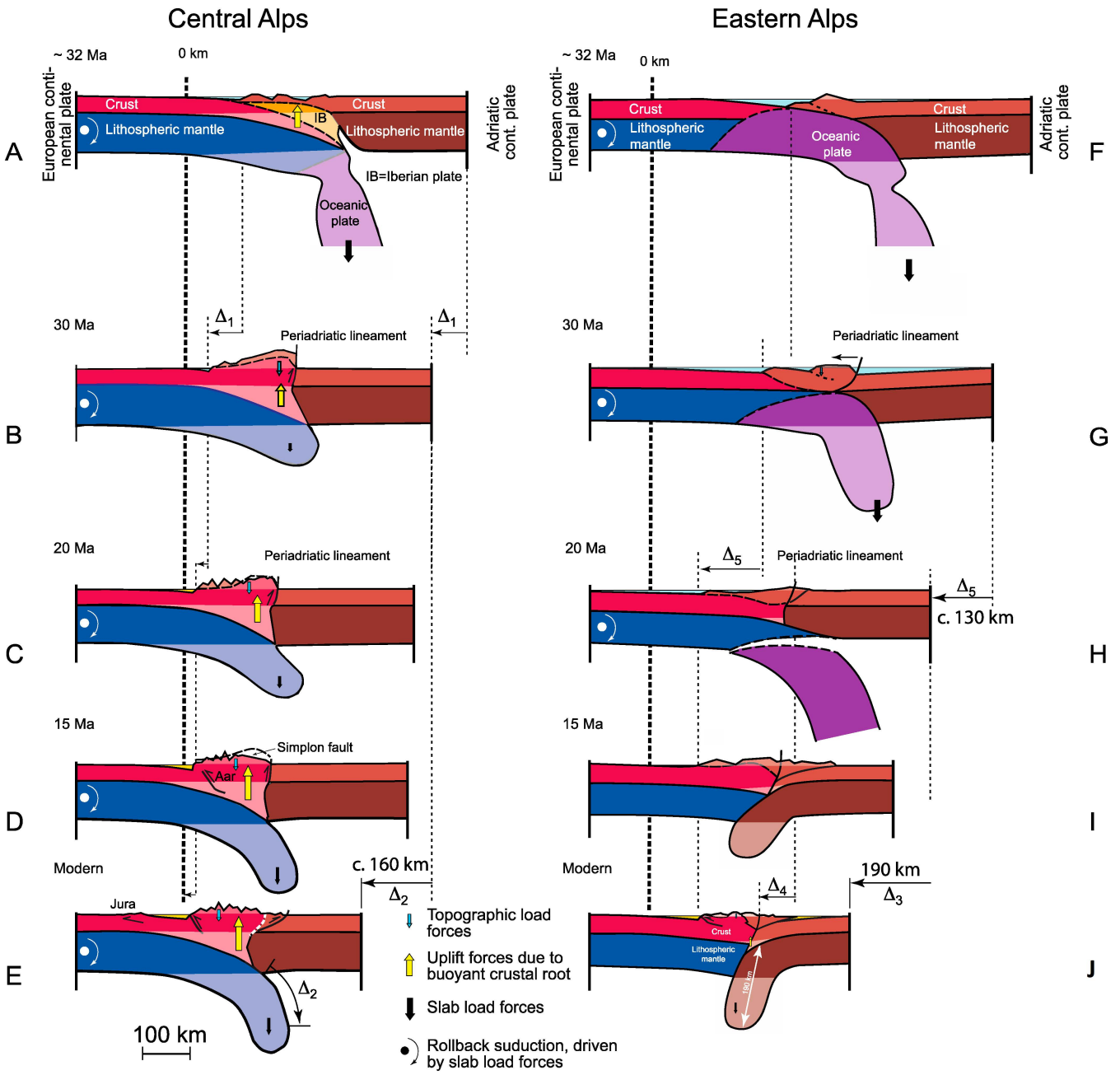

Figure 7. Tectonic evolution of the Alps. See Figure 2 for location of cross sections. (**A**) At 35–32 Ma, the Iberian plate was accreted to the Central Alps, forming a stack of buoyant crustal rocks. The oceanic slab, which has a high density, and which deflected the foreland plate towards the South, was still attached to the European plate. (**B**) At 32–30 Ma, the resistance of the crustal root to enter the subduction channel resulted in slab-breakoff where the dense oceanic slab was removed from the continental plate. This latter plate experienced a rebound because of the removal of the downward-directed slab force and driven by the buoyancy of the crustal root. The result was the incipient rise of the Alpine topography between 30–25 Ma. (**C**–**E**) After 30 Ma and beneath the Central Alps, the lithospheric mantle slab has continued to be delaminated from the continental crust and to be subducted but remained attached to the European plate. Beneath the Eastern Alps (**F**), no Iberian crustal rocks were accreted, and buoyant material was largely missing. The oceanic part of the European plate was attached to the continental plate and deflected the foreland plate towards the south.

(**G**) At 30 Ma, the oceanic slab was still attached to the European plate, causing a southward-directed flexure of this plate. (**H**) The subducted oceanic part of the European plate became detached at c. 20 Ma beneath the Eastern Alps [40] causing a rebound of the foreland plate, but not as much as in the Central Alps because there existed only a small buoyant crustal root. (**I**,**J**) Beneath the Eastern Alps the removed European oceanic slab was eventually replaced by the slab of the Adriatic plate after 20 Ma.

Because the Alpine front did not significantly propagate farther into the foreland after 20 Ma [73], the northward shift of the Periadriatic lineament had to result in a shortening of the Austroalpine nappes and the underlying European continental crust. Upon restoring the cross-section of Figure 4B, we infer that this was accommodated by a combination of (i) stacking of European crustal rocks beneath the Tauern window resulting in a doubling of the European crust along our section in Figure 4B [36], and of (ii) east-directed lateral extrusion of the Eastern Alps through left- and right-lateral faulting (Linzer et al. [59], see their Figure 10). Antiformal stacking of the European crustal rocks [87] beneath the Tauern window was also associated by tectonic exhumation. This was accomplished through low-angle normal faulting along the Brenner and Katschberg faults (BF and KF in Figure 2) [36] that border the Tauern window on the western and eastern margins, respectively. The contemporaneous occurrence of crustal stacking, tectonic exhumation and lateral extrusion renders the budgeting of the relative contributions of these processes to the N-S shortening along a cross-section rather complicated (see Figure 8 in Rosenberg et al. [36]). Therefore, upon restoring the section through the Eastern Alps, we considered that most of the antiformal stacking records a shortening contribution of c. 39 km [35] and occurred in response to the post-20 Ma northward indentation of the Adriatic plate [36]. Accordingly, the rest of the 70–80 km of N-S shortening between the Periadriatic lineament and the orogen front (Δ_4 in Figure 7J) was possibly accommodated by E-directed lateral extrusion of the Eastern Alps through left-lateral and right-lateral faulting.

In contrast to the aforementioned scenario, the pre-20 Ma shortening in the Eastern Alps is rather poorly constrained, because limited surface and subsurface information exists to estimate the details of the tectonic architecture beneath the core of the Eastern Alps [35]. Therefore, and similarly to our previous restoration for the Central Alps [33], we used the progradation of the northern Alpine front (Δ_5 in Figure 7H, based on Kuhlemann and Kempf [80]) as constraints to estimate the amount of rollback subduction. We thereby infer that the upper crustal rocks of the Adriatic plate were passively riding on top of the collisional zone when the oceanic part of the European plate was subducted, and that the Adriatic plate experienced only a limited amount of internal shortening during this time (Figure 7F,G). Note that the depth at which the lower part of the oceanic plate was delaminated at c. 32 Ma beneath the Eastern Alps is partly based on a restoration by Handy et al. [32].

3.2. Subsidence History and Evolution of the Molasse Basin

We compiled stratigraphic, provenance and sedimentologic data from various sources into a synthesis of how the Molasse basin evolved at a large scale and through time. Here, we mainly focused on the time that is recorded by the time interval that chronicles the development from the Lower Marine Molasse to the Upper Freshwater Molasse group (Figure 6) because the chronologic constraints are relatively precise for these units. We also compiled stratigraphic data that allowed us to determine the subsidence history in the various portions of the basin. We particularly used data on the thicknesses of strata, together with published estimates of paleo-water depths for these units to reconstruct the subsidence of the foreland plate. In the Austrian, German and Swiss parts of the Molasse basin, the sites for which we conduct these analyses are situated in the foredeep part adjacent to the current orogenic front. The corresponding sites are labelled as A (Austrian Molasse), G (German Molasse) and S (Swiss Molasse) in Figure 2. These portions of the basin were not situated in a wedge-top position. Therefore, the subsidence patterns that we

approximate for these segments were not influenced by syn-depositional thrusting [14,19]. The situation is more complicated for the French part of the basin (site labelled as F in Figure 2), because a large portion of the sediment accumulated in a wedge-top position [21], and sediment accumulation in more distal parts of the basin were partly controlled by the opening of the Bresse graben (Figure 2). Therefore, we selected the region immediately NE of Chambery in the Rumily syncline (Ru in Figure 2) for our analysis because detailed chronologic data has been established for this area (see below and [21]). Furthermore, this site is located adjacent to the Alpine thrust front and is, from this point of view, in a similar position to the other sections, which will facilitate the comparison of the inferred subsidence rates between the sites. Finally, as will also be explained further below, the Rumily area was most likely situated in a basin-marginal position during Late Oligocence times [80]. Therefore, the occurrence of a first distinct subsidence pulse would possibly indicate a change in the geodynamic mechanisms. Note that compaction of sediment and porosity loss was not considered in these calculations. To account for this possible drawback, we considered an uncertainty of several hundred meters for the estimates of the depth of the foreland plate, and of several 100 ka for the time when these depths were reached. We acknowledge that this approach is simplistic, but it is precise enough to allow a comparison of the subsidence trends between the different portions of the basin, which is the scope of this paper.

3.2.1. French Part of the Molasse Basin

The chronologic and stratigraphic record of Molasse deposits exposed in the Rumily syncline (Table 1) is based on a combination of sedimentologic, sequence stratigraphic, seismo-, chemo- and bio-stratigraphic data, and some sections have been calibrated with magnetostratigraphy by Kalifi and coauthors [21] (see Figure 13 in [21]). We also used the data of the aforementioned authors as constraints for estimating the propagation rates of the thrust front as this is based on detailed palinspastic restorations of shortening within a well constrained chronological framework. The position of the Alpine thrust front and the distal basin at c. 35 Ma is taken from Kempf and Pfiffner [88].

Table 1. Source information that was used to calculate the subsidence pattern of the foreland plate underlying the Western (French) part of the Molasse basin NE of Chambery (site labelled as F in Figure 2). USM = Lower Freshwater Molasse, OMM = Upper Marine Molasse, OSM = Upper Freshwater Molasse; these are the commonly used German abbreviations for the Molasse groups.

Lithostratigraphic Unit	Ages (Ma)	Thickness (m)	Water Depth (m)	Proxy for Depth of Foreland Plate (m)	References
USM	30–21	50	0	50	Kalifi et al. [21]
OMM	21–18	200	20	270	Kalifi et al. [21]
OMM	20–17	500	20	770	Kalifi et al. [21]
OMM	17–16.5	270	20	1040	Kalifi et al. [21]
OMM	16.5–14	300	0	1320	Kalifi et al. [21]
OSM continued (?)	14–10	250	0	1570	
Erosion (?)	10–0	100	0	1470	

In this part of the basin, the sediments were mainly deposited in a wedge-top depozone position. Because the thrust front advanced towards the west through time, the facies relationships are strongly heterochronous, and the sites of highest sediment accumulation shifted towards the West as thrusting proceeded. Therefore, for the Rumily syncline, we expect a combination of a positive subsidence signal controlled by the loading through orogenic processes and subduction tectonics, and a negative component in response to the piggy-back displacement of the basin along SE dipping ramps. Mapping of angular unconformities within a chronological framework revealed that this part of the basin entered into a piggy-back position after c. 17.5 Ma [21]. The analysis also disclosed that sediment accumulation rates and hence the subsidence rates of the basin experienced a

rapid increase at 18 Ma at the latest, and that high sediment accumulation rates persisted despite the occurrence of a negative component in response to the piggy-back displacement of the depositional realm.

3.2.2. Swiss Part of the Molasse Basin

For the Swiss segment of the Molasse basin, data on the stratigraphic architecture are taken from a site labelled as S in Figure 2 and are based on various sources that are listed in Table 2. The uncertainty on the age model is c. ±1 Ma, and an uncertainty of ±150 m has to be considered for the depth of the bedrock underlying the Molasse sequences. This information is valid for the Plateau Molasse in the Lucerne area (Figure 2). The propagation rate of the thrust front is taken from a previous publication of the authors of this work [26]. The chronological framework of the Swiss part of the Molasse basin is based on magnetopolarity stratigraphies [14,16,17,89,90]. Van der Boon et al. [90] present a chronological framework where the transition from the Lower Marine Molasse to the Lower Freshwater Molasse is c. 2–3 Ma older than proposed before [14,16,89]. However, we tentatively prefer the original [14,16,89] chronological framework because it is a best-fit correction between magnetostratigraphic chronologies of several sections and the mammal biostratigraphic framework established for the Molasse basin and the surrounding sedimentary troughs [91]. It is thus founded on a broader dataset than the chronological framework for the transition from the Lower Marine Molasse to the Upper Freshwater Molasse by Van der Boon et al. [90], which is based on the nannoplankton records and one section with three reversals only. In addition, Van der Boon et al. [90] mentioned that an age of c. 30 Ma for the transition from the Lower Marine Molasse to the Lower Freshwater Molasse is also possible.

Table 2. Source information that was used to calculate the subsidence pattern of the foreland plate underlying the Swiss part of the Molasse basin near Lucerne (see site labelled as S in Figure 2 for location). UMM = Lower Marine Molasse, USM = Lower Freshwater Molasse, OMM = Upper Marine Molasse, OSM = Upper Freshwater Molasse; these are the commonly used German abbreviations for the Molasse groups.

Lithostratigraphic Unit	Ages (Ma)	Thickness (m)	Water Depth (m)	Proxy for Depth of Foreland Plate (m)	References
UMM	32–30	150	50 m at 30 Ma	200	Diem [92] Schlunegger et al. [14]
USM I	25–20	500	0	650	Schlunegger et al. [14] Kempf et al. [16]
USM II	25–20	1460	0	2110	Schlunegger et al. [14] Kempf et al. [16]
OMM I	20–18	600	20	2730	Schlunegger et al. [14]
OMM II	18–16.5	225	50	2985	Schlunegger et al. [14]
OSM preserved	16.5–15.5	500	0	3435	Schlunegger et al. [14]
OSM continued	15.5–10/5	1400–3000 mean 2350	0	5785	Cederbom et al. [83]
Erosion	10/5–0	1400–3000 mean 2350	0	3435	Cederbom et al. [83]

3.2.3. German Part of the Molasse Basin

The stratigraphic framework of the German Molasse basin (Table 3) is mainly taken from the results of the stratigraphic analyses of drillhole data (drillhole A in Jin et al. [81] that is situated 30 km SSE of Munich; see site labelled as G in Figure 2) and seismic lines [81,82]. Therefore, this section is situated in the northward extension of the Giudicaria fault and will offer information about the transition from the central to the eastern part of the foreland trough. We selected the most proximal section of Jin et al. [81] for the purpose of comparison with the Swiss, Austrian and French parts of the Molasse basin where we also focused on changes of the subsidence rates for sites as close to the modern

Alpine thrust front as possible. Note that because the sediments were mainly deposited in a coastal environment, we considered water depths between 50 and 20 m for our analyses. In addition, eustatic variations in sea level were not considered in these analyses because they were significantly less than the changes in accommodation space caused by tectonic subsidence [81,82].

Table 3. Source information to infer the subsidence of the foreland plate underlying the German part of the Molasse basin (see site labelled as G in Figure 2). OSM = Upper Freshwater Molasse.

Lithostratigraphic Unit	Ages (Ma)	Thickness (m)	Water Depth (m)	Proxy for Depth of Foreland Plate (m)	References
Rupelian marls	32–30	800	50 m at 30 Ma	850	Jin et al. [81]
Chattian marls and sands	30–25	1700	50	2550	Jin et al. [81]
Aquitanian marls and sands	25–20	1300	50	3850	Jin et al. [81]
Sandstone-shale Series; Fish Shales	20–18	150	20	3970	Jin et al. [81]
Neuhofer beds, Blättermergel and Glauconite sands	18–16.5	250	20	4220	Jin et al. [81]
Kirchberger beds and OSM	16.5–12	450	0	4650	Jin et al. [81]
OSM continued	12–10/5	600	0	5250	Lemcke [85]
Erosion	10/5–0	600	0	4650	Lemcke [85]

3.2.4. Austrian Part of the Molasse Basin

For the Austrian segment of the Molasse basin, data on the stratigraphic architecture are based on various sources that are listed in Table 4. These data have been established for the part adjacent to the orogen front between Salzburg and Linz (Figure 2, site labelled as A). The uncertainties on the age model range between ±1 Ma and ±2 Ma, and an uncertainty of ±250 m has to be considered for the depth of the plate underlying the Molasse sequences. Data on the propagation rate of the thrust front was taken from a synthesis article [80].

Table 4. Source information that was used to calculate the subsidence pattern of the foreland plate underlying the Austrian part of the Molasse basin near Salzburg (see site labelled as A in Figure 2 for location).

Lithostratigraphic Unit	Ages (Ma)	Thickness (m)	Water Depth (m)	Proxy for Depth of Foreland Plate (m)	References
Schöneck, Dynson, and Eggerdingen Fms.	35–30	65	600	665	Sachsenhofer et al. [93]
Zupfing Fm.	30–27	450	400–600 (mean of 500)	1015	Sachsenhofer et al. [93]
Puchkirchen Fm. and sands	27–20	1500	1000–1500 (mean of 1250)	3265	Bernhardt et al. [94] Grunert et al. [95]
Hall Fm. and Innviertel group	20–16.5	1200	50	3265	Hülscher et al. [19]
OSM	16.5–10	c. 450	0	3665	Ruig and Hubbard [96]
Uplift and erosion	5–0	c. 300	0	3365	Lemcke [85]

4. Results

4.1. Sequential Restoration of the Alps and Orogenic Development

The sequential restoration of the simplified cross-sections illustrated in Figures 3B and 4B through the Central and Eastern Alps allowed us to reconstruct the position of the subducted

lithospheric mantle slab for different time intervals and to propose a scenario of how the Central and Eastern Alps, and partially also the Western Alps, evolved through time (Figure 7). In the Western and Central Alps, the Tertiary subduction of the crystalline basement of a narrow and elongated eastward extension of the Iberian plate (Figure 7A) to greater depths resulted in blueschist metamorphic conditions with pressures up to 10 kbar [97], while the sedimentary cover was detached and thrusted to the north, forming the Penninic sedimentary nappes (Figure 2). The subduction of Iberian crustal material also resulted in the incipient growth of the buoyant crustal root, which currently maintains the topography of the Central and Western Alps at high elevations [46,47]. In the Eastern Alps, however, subduction of the European oceanic lithosphere beneath the Adriatic continent and closure of the Piemont Ocean continued for some time, and no thick crustal root was formed.

Between 35 and 32 Ma, the buoyant European continental lithosphere with a lower flexural rigidity than the previously subducted oceanic lithosphere slab started to enter the subduction channel beneath the Western and Central Alps (Figure 7A). This resulted in extensional forces and eventually in slab breakoff between 32 and 30 Ma [98]. The removal of the subducted oceanic lithosphere increased the relative importance of the buoyancy versus the slab load forces, thereby lifting the surface of the Alps to the current altitudes within a few million years [26,27]. Uplift was accommodated by backthrusting along the Periadriatic lineament (Figure 7B,C) [99], which delineated the orogen front on the retro side at that time and which also served as a pathway for the intrusion of the Bergell and Adamello plutons [34] (labelled as Be and Ad on Figure 2). As a further consequence, slab breakoff resulted in the advection of heat, which resulted in the Barrovian-type metamorphism of rocks (temperatures up to 670 °C) between 25 and 20 Ma particularly in the southern limb of the Penninic rocks (Lepontine Dome) north of the Periadriatic fault [100,101].

In the Eastern Alps, however, part of the oceanic lithosphere remained attached to the European continental plate (Figure 7F,G) until c. 20 Ma, when it started to tear from its continental part (Figure 7H). Tearing most likely proceeded from the West to the East [37] and was associated with a major segmentation of the Eastern Alps through left-lateral faulting [42,43]. The inferred slab breakoff was also coeval with N-directed thrusting and shortening in the Western Carpathians [102,103] and eventually lead to the slab tearing around the Carpathians [57]. It was additionally considered to offer space for the counterclockwise rotating Adriatic plate [37] to subduct towards the North, thereby initiating the deformation of Southern Alps [40,59] and offsetting the Periadriatic lineament through left-lateral slip along the Giudicaria fault [34]. This was also the time when the propagation rates of the Eastern Alpine front rapidly decreased [73] and came to halt a few Mys after 20 Ma (Figure 7I,J) [73]. In the Western and Central Alps, however, the post-30 Ma European lithosphere slab remained attached to the European plate. Ongoing slab rollback subduction of this plate [33] continued to control the tectonic processes on the surface and the deformation on the northern margin, which propagated into the foreland and resulted in the folding of the Jura fold-and-thrust belt from c. 10 Ma onward (Figure 7E) [104].

4.2. Development and Subsidence of the Molasse Basin between 35 and 20 Ma

The entrance of the European continental crust into the subduction channel at c. 35 Ma is considered to mark the initiation of the basin on the northern side of the Alps as a foreland basin. At that time, turbidity currents with sources in the Adriatic continental plate resulted in the deposition of submarine fans (e.g., North Helvetic Flysch; Figure 8A) along the Alpine thrust front between the Western and Central Alps. The built up of andesitic volcanoes on the Adriatic plate resulted in the admixture of some volcanoclastic material in the Flysch trough [105,106]. The transport of sediment was spatially constrained and occurred from the West to the East in a deep trough. East of Munich, the deep marine Flysch lobes transitioned into a pelagic sedimentary realm (Figure 8A).

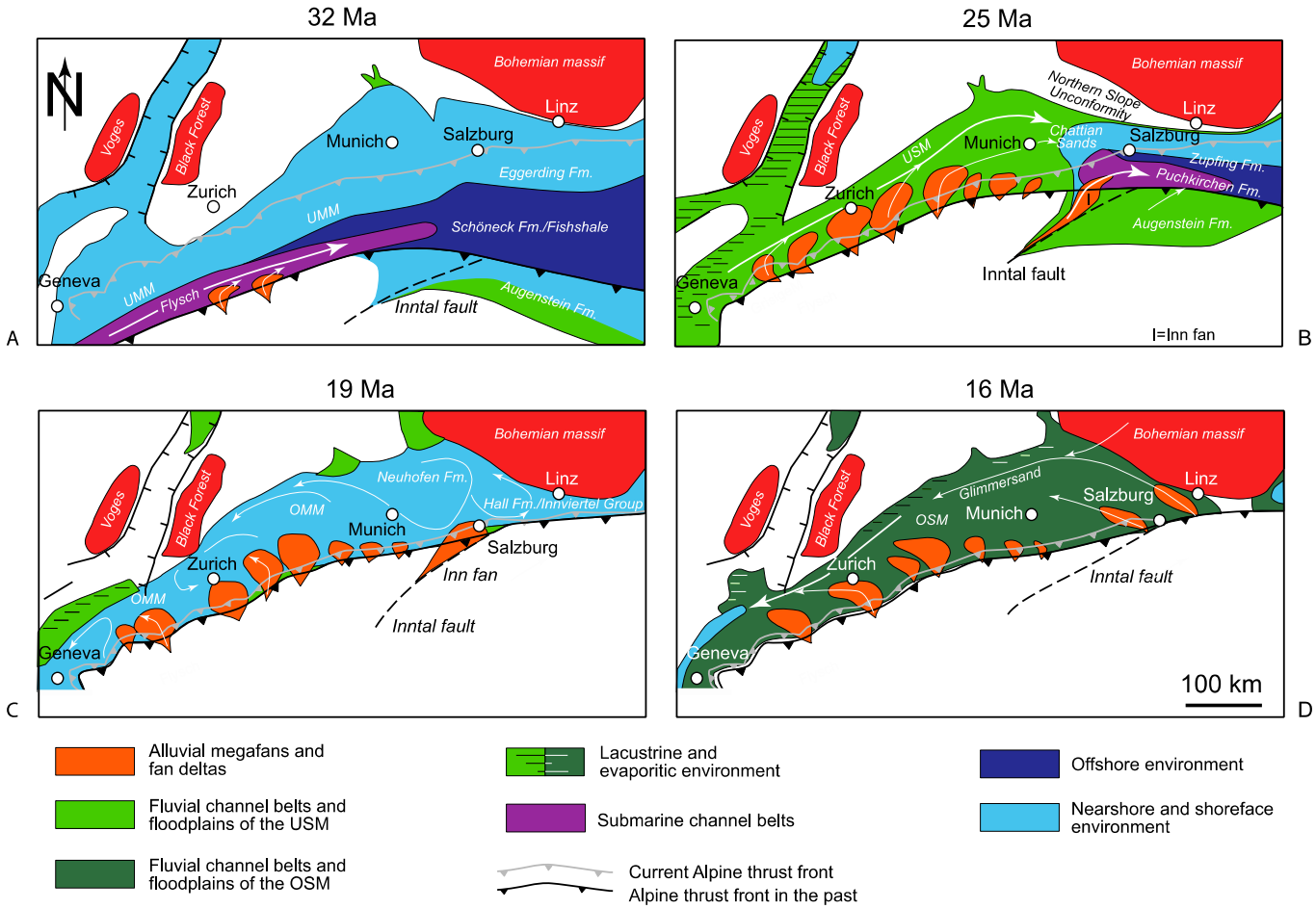

Figure 8. Paleogeography of the Molasse basin. (**A**) Situation at 32 Ma, when the basin axis was occupied by a Flysch trough. Turbidity currents routed the clastic material with sources in the Adriatic continent to the Austrian part of the basin, where offshore marine conditions prevailed. (**B**) The situation changed after 30 Ma, when large sediment fluxes from the rising Alps resulted in overfilled conditions in the central part of the Molasse basin, giving way to the accumulation of the Lower Freshwater Molasse group (USM). The western part was characterized by basin-marginal facies at that time. The fluvial systems in the central Molasse transported the clastic material until the area near Munich, where the terrestrial facies transitioned into the deep Flysch trough of the eastern (Austrian) Molasse basin. There, the largest portion of the supplied sediment was derived from the area near the Periadriatic fault and transported via the paleo-Inn valley into the Flysch trough, as recent provenance tracing has shown [20]. Thick fluvio-deltaic sediments with sources in the adjacent orogen accumulated in a wedge-top position (Augenstein Formation). (**C**) At 19 Ma the eastern Molasse basin became filled and finally transitioned from the Flysch to the Molasse stage, here represented by the Upper Marine Molasse group (OMM). The depositional ream of the Augenstein Formation was uplifted, and its material became eroded and re-deposited to form the rapidly prograding Hall Formation. (**D**) The entire basin was overfilled during the deposition of the Upper Freshwater Molasse group (OSM), and the sediment was transported towards the West. This suggests a reversal in the drainage direction, which occurred during deposition of the Upper Marine Molasse group. Updated and modified from Kuhlemann and Kempf [80]. Reproduced with permission by Elsevier (license number 5315851404282).

At c. 32–30 Ma, the inferred occurrence of slab breakoff beneath the Western and Central Alps [34] and the resulting rise of the Alpine topography occurred at the same time when the deposition of the North Helvetic Flysch gave way to the regressive sequence of the Lower Marine Molasse group (UMM; Figure 9A,B), which subsequently transitioned into

the prograding fluvial systems of the Lower Freshwater Molasse group (USM) sometime before 30 Ma. Overfilled conditioned prevailed between 30 and 20 Ma, when large streams with sources in the high Alps shed their material to the basin, thereby forming megafans at the thrust front that interfingered with an axial drainage in the basin's axis (Figure 8B).

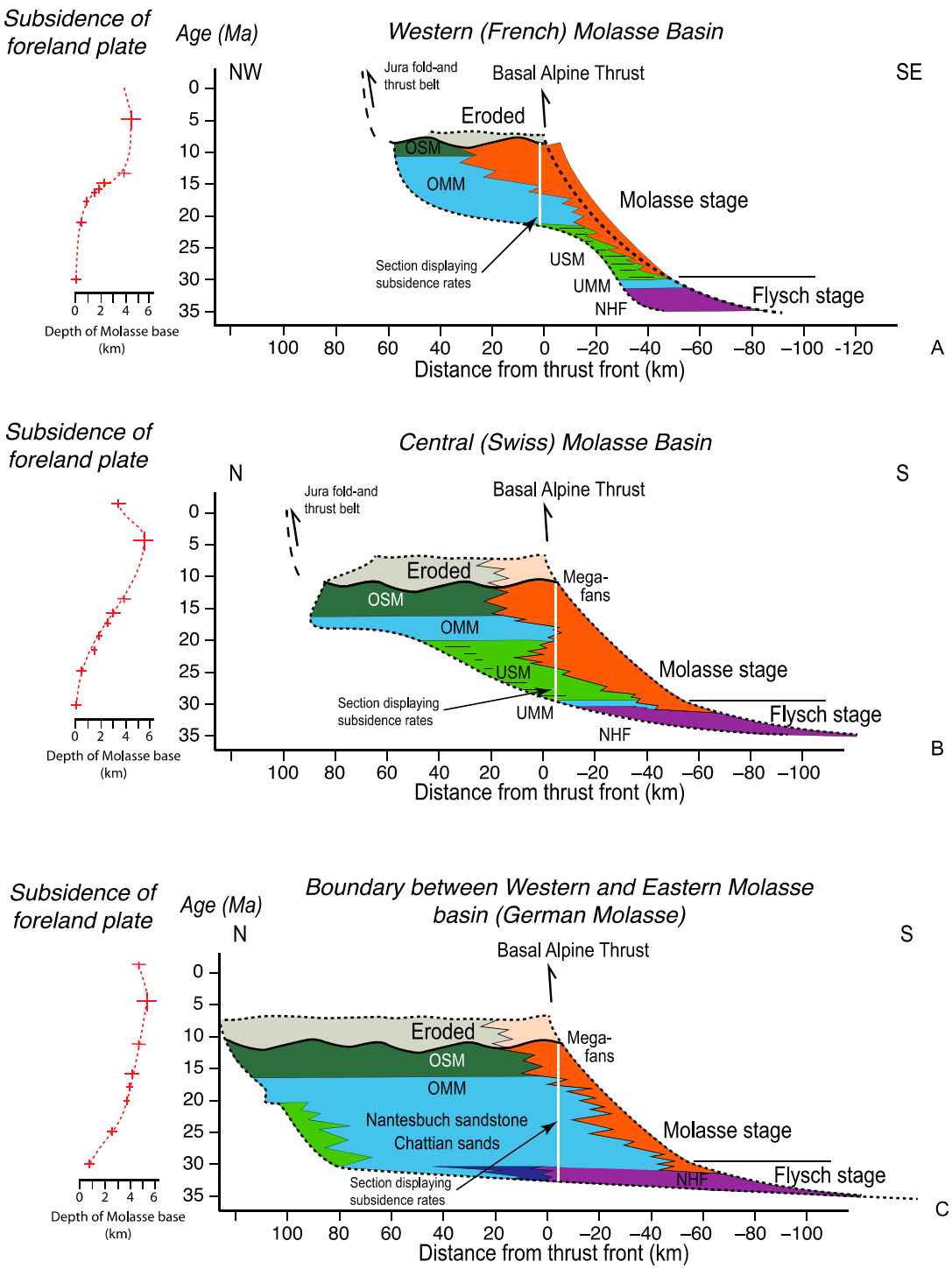

Figure 9. *Cont.*

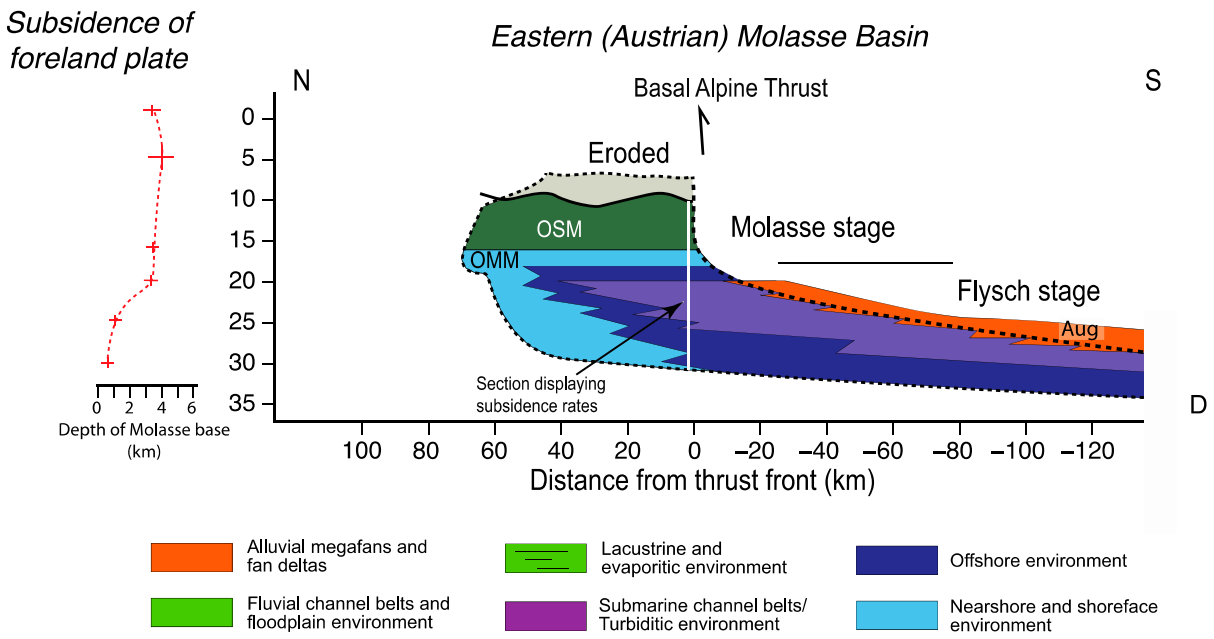

Figure 9. Subsidence pattern of the Molasse basin within a temporal framework. Because the sections are situated in the Plateau Molasse adjacent to either the Basal Alpine thrust (Austrian and French Molasse) or to the front of the Subalpine Molasse, the deflection of the foreland plate was only marginal in these areas at 30 Ma and before. (**A**) Chronological diagram for the Western (French) Molasse basin near Chambery at the site labelled with F in Figure 2 (Table 1). Sedimentation occurred in a wedge-top position at the proximal basin border. The transition from the Flysch to the Molasse stage occurred at c. 30 Ma, and the propagation rate of the Alpine thrust front was nearly constant between 30 and 5 Ma. After 20 Ma, the distal basin border was defined by the western limit of the Bresse graben (Figure 2). Before 20 Ma, the subsidence rates of the foreland plate in this part of the basin were negligible. They started to increase after 20 Ma. (**B**) Chronological diagram for a section across the Central (Swiss) Molasse basin near Lucerne (see site labelled as S in Figure 2 and Table 2). The transition from the Flysch to the Molasse stage occurred at c. 30 Ma. The propagation rate of the Alpine thrust front decreased at c. 30 Ma. In the basin axis, the subsidence rates of the foreland plate continuously increased. (**C**) Diagram for the boundary between the eastern and western Molasse basin near Munich (site labelled as G in Figure 2). The subsidence pattern was taken from the data displayed in Table 3. The basin evolution shares similarities to the Swiss and Austrian portions of the Molasse basin. Similar to the Swiss basin, the transition from basin underfill to overfill occurred at c. 30 Ma. However, the subsidence history can be compared with the Austrian basin in the sense that the subsidence rates where high before 20 Ma, after which they slowed down. (**D**) Chronological diagram for a section across the eastern (Austrian) Molasse basin near Salzburg (see Table 4 for database, and site labelled as A in Figure 2). The time between 30 and 20 Ma was characterized by a rapid northward propagation of the Alpine thrust front. The fluvio-deltaic sediments of the Augenstein Formation (Aug) accumulated in a wedge-top position. At 20 Ma, the Austrian Molasse basin transitioned from the underfilled Flysch stage into the overfilled Molasse stage, and the deformation at the Alpine thrust front came to a halt shortly after 20 Ma. The distal basin border was most likely limited by a Hercynian fault, which currently separates the Bohemian massif from the Molasse basin (Figure 2). In the area north of the modern Alpine front, the subsidence rates of the foreland plate increased until 20 Ma. After that time, the subsidence rate was constant and nearly negligible. NHF = North Helvetic Flysch, UMM = Lower Marine Molasse, USM = Lower Freshwater Molasse, OMM = Upper Marine Molasse, OSM = Upper Freshwater Molasse.

Sediment thicknesses together with the size and number of fluvial channels increase as far east as Munich (Figure 10A), where the fluvial deposits of the Lower Freshwater Molasse transitioned into a coastal environment (Chattian Sands and Nantesbuch Sandstones) and

finally into deep marine submarine fans in the Austrian Molasse (Zupfing Formation, c. 30–27 Ma; and Puchkirchen Formation, c. 27–19.6 Ma; Figures 8B and 10A,B). There, the shift towards more coarse-grained material at the boundary between the Zupfing and Puchkirchen Formations [19] possibly reflects the response to the larger supply of sediment from the rising eastern margin of the Central Alps, as U-Pb and cooling ages of detrital zircon minerals imply [20]. Please note that we consider the region west of the Tauern window, which was the source area of the Puchkirchen Formation [20], and thus also the region west of the Giudicaria fault as part of the Central Alps.

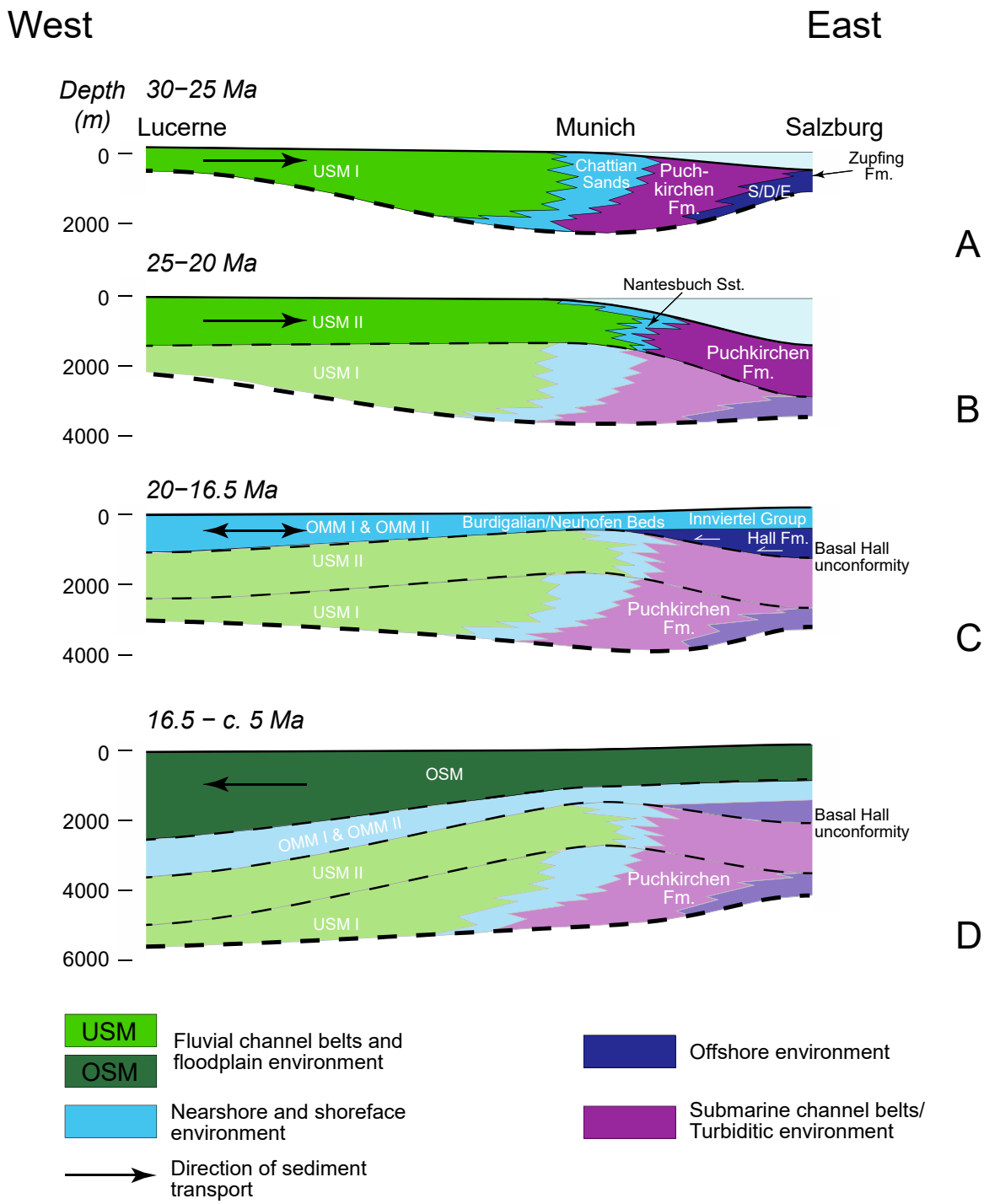

Figure 10. Subsidence of the Molasse basin for a section along the topographic axis. (**A**) Situation between 30 and 25 Ma. This was the time when the sediments of the USM I (lower part of the Lower

Freshwater Molasse group) were deposited in the central Molasse basin. The fluvial facies of the USM I then transitioned into a Flysch trough farther east of Munich. (**B**) Situation between 25 and 20 Ma, when the Flysch trough in the eastern part of the basin started to subside very rapidly, possibly driven by rapid rollback subduction and the related northward propagation of the orogen (see Section 5.3). The central portion of the Molasse basin was still occupied by fluvial systems, which resulted in the accumulation of the USM II (upper part of the Lower Freshwater Molasse; Figures 5 and 6). (**C**) Situation when the sediments of the Upper Marine Molasse (OMM) were deposited. The subsidence in the eastern Molasse basin became nearly to a halt, whereas the foreland plate beneath the central Molasse basin continued to subside. (**D**) During the deposition of the Upper Freshwater Molasse group (OSM), the subsidence rates of the foreland plate were much higher in the western/central part than in the eastern Molasse. As a consequence, the sediment dispersion occurred to towards the West. USM = Lower Freshwater Molasse, OMM = Upper Marine Molasse, OSM = Upper Freshwater Molasse, S/D/E = Schöneck, Dynow and Eggerding Formations. The arrows indicate the direction of sediment transport in the basin axis.

It was proposed that a valley following the Inntal fault served as pathway for the sedimentary material in the Puchkirchen Formation [20]. Although the major deformation along such faults occurred after 20 Ma, the occurrence of earlier movements along them cannot be excluded [107]. Additionally, in the eastern Molasse basin, sedimentation at the proximal basin border occurred in a wedge-top position where the >1000 m-thick fluvio-deltaic deposits of the Augenstein Formation [108] sealed the Alpine thrust front (Figure 8B). In contrast, the western part of the foreland basin (Chambery-Geneva area) was characterized by the deposition of gypsiferous marls, red sandstones, freshwater carbonates and paleosoils [109–111], suggesting a sedimentary environment that is indicative for a basin margin [80,110]. This facies assignment is corroborated by the low subsidence rate of <50 m/Ma in the western Molasse. This rate then increased to c. 200 m/Ma towards the central Molasse basin and finally to >400 m/Ma in the eastern Molasse particularly between 25 and 20 Ma (Figure 9). The eastward trend towards higher subsidence rates was additionally associated with an increase in the propagation rate of the Alpine thrust front from <3 km/Ma in the western basin to c. 6 km/Ma in the central basin and finally to >10 km/Ma in the eastern Molasse basin (Figure 9).

4.3. Development and Subsidence of the Molasse Basin after 20 Ma

The situation changed at c. 20 Ma, when the coarse-grained Puchkirchen submarine fan system in the Austrian Molasse became finer grained and then transitioned, after 19 Ma, into the prograding prodelta deposits of the Hall Formation and finally into the shallow marine environment of the Innviertel Group (Figures 8C, 9D and 10C). This change from deep to shallow marine conditions occurred within less than 2 My and was recorded by the N-directed clinoforms of the Hall Formation that onlap onto the Puchkirchen submarine fan deposits, thereby forming the Base Hall Unconformity [19] (Figure 10C). This suggests the occurrence of a large sediment pulse possibly in response to the uplift and erosion of the wedge-top deposits of the Augenstein Formation [20], which became eroded and redeposited in the Austrian Molasse at that time [20,108].

The shallow marine and tidally dominated environment of the Innviertel Group then evolved into the fluvial conditions of the Upper Freshwater Molasse group at approximately 16.5 Ma (Figures 8D, 9D and 10D), when sediment dispersal occurred towards the West. Additionally, at 20 Ma, the subsidence rate of the eastern foreland plate decreased to <50 m/My, and the Alpine thrust front came to a halt shortly after 20 Ma [73] (Figure 8C). This change from an East-directed sediment transport on the deep marine submarine fan system to the N-directed progradation of the post 19 Ma-old prodelta deposits and finally to the West-directed sediment dispersal during OSM times thus points both towards a shift from basin underfill to overfill and towards a reversal of the drainage direction (Figures 8 and 10).

Such a change in the sediment dispersion is also recorded in the Swiss Molasse basin. There, the fluvial environment of the Lower Freshwater Molasse (Figure 8) with an E-directed discharge transitioned into the shallow marine environment of the Upper Marine Molasse (OMM) at 20 Ma. A second transgression at 17.5 Ma started in the western part of the Swiss Molasse basin and proceeded towards the East. This suggests that the basin adapted a westward-directed tilt after 18 Ma [112], which is consistent with the aforementioned observations from the Austrian Molasse (Figures 8 and 10). After 16.5 Ma, progradation of alluvial megafans finally resulted in the re-establishment of terrestrial conditions in the Molasse basin, giving way to the construction of the Upper Freshwater Molasse group. Between 16.5 and c. 10 Ma, sedimentation continued in terrestrial conditions, and streams with sources in the Eastern Alps and the Bohemian massif (Glimmersand) converged with streams from the Central Alps in the Swiss Molasse basin and finally discharged via the Bas-Dauphine basin and the Rhône Graben in France to the Mediterranean (Figure 8D). In contrast to the eastern Molasse basin, the subsidence rates of the central foreland plate continuously increased after 20 Ma, reaching a value of c. 400–500 m/My between 20 and 15 Ma, and the deformation front continued to propagate towards more distal sites (Figure 9). A similar yet much higher increase in sediment accumulation rates is also recorded in the western Molasse basin. There, shallow marine sediments started already in the Aquitanian. Deposition of Molasse sediments occurred in wedge-top and foredeep positions, and the depocenters migrated westward together with the thrust front. At 18 Ma, and thus contemporaneously with the inferred drainage reversal, the western Molasse basin experienced a rapid increase in sediment accumulation rates from <150 m/My to >1000 m/My (Figure 9A). The entire basin then became uplifted and eroded sometime between 10 and 5 Ma [71,83].

5. Discussion

The stratigraphic development of the Molasse Basin and particularly the transition from marine to terrestrial conditions has commonly been related to periods of thrusting and surface loading at the orogen front [6,13–16,81,82], or to changes in the eustatic sea level [81,82,92,113]. However, excluding the transition from basin underfill to overfill [105] which occurred at c. 30 Ma in the central Molasse basin, the control of slab loads on the stratigraphic development of the Molasse basin have received much less attention in the literature [28]. Here, we first discuss whether topographic loads and the loads of the sedimentary fill of the Molasse basin had the potential to contribute to the formation of accommodation space in the basin itself. We continue with outlining how changes in the eustatic sea level potentially influenced the formation of distinct sedimentary cycles in this basin. In the last section, we then elaborate how the subduction processes at deeper lithosphere levels beneath the Western-Central and Eastern Alps (Figure 7) potentially impacted the generation of the sediment in the Alpine hinterland and the routing of the sedimentary material in the Molasse foreland basin (Figures 8–10).

5.1. Possible Controls of Surface and Basin Fill Loads on the Development of the Molasse Basin

It was proposed that the sedimentary loads of the basin fill (Figure 1) potentially contribute to a widening of a foreland basin, e.g., [114]. Such an interpretation is based on the results of flexural models that were designed to explore the basin response to the combined effect of crustal thickening in the orogen and the erosional redistribution of surface loads from the orogen to the foreland basin [6,8]. According to these models, a basin load control on the widening of the foreland trough is a valuable interpretation provided that there is compelling evidence for surface loads to exert a measurable impact on the basin's subsidence history. In this context, the stacking of European crustal material beneath the Tauern window was considered to have contributed to the formation of such surface loads. According to flexural models, the basin is expected to respond to such crustal stacks by a period of rapid subsidence, as proposed by, e.g., Rosenberg et al. [36]. In particular, these authors interpreted that the thickening of the Molasse deposits from Salzburg to

Munich reflects the occurrence of a corresponding trend in crustal loads where the stack of European crustal material appears to be thinner in the eastern than in the western part of the Tauern window. However, according to our restoration of the geodynamic processes, the buildup of the antiformal stack underneath the Tauern window occurred at the highest rates when the tectonic component of the basin's subsidence nearly came to a halt, which was the case after 20 Ma (Figure 9D). Therefore, we do not consider that the along-strike differences in the crustal thicknesses beneath the Tauern window had a large impact on the formation of the accommodation space in the Molasse basin. In the same sense, it was proposed that the uplift of the Aar massif at c. 20 Ma caused an increase in the surface loads and, as a consequence, a subsidence pulse in the Swiss part of the Molasse basin [6]. However, there is no evidence for such a basin response in the subsidence history of the basin (Figure 9B). Additionally, for the Swiss part of the Molasse basin, Schlunegger and Kissling [26] identified a disconnection between the development of the Alpine topography and the formation of accommodation space in the basin. Based on their conclusion we thus infer that surface loading in the Alps was not the primary driving mechanism for the deflection of the foreland plate. Admittedly, a recent research contribution documented that the Alps reached a high topography during Miocene times [115] particularly in the hangingwall area of the Simplon fault (Figure 2). However, these high elevations were possibly local in nature [115] and could have reflected a transient state in the rearrangement of the Alpine drainage network, which started at c. 20 Ma [116–118]. In addition, at the same time, tectonic exhumation in the Lepontine area through slip along the Simplon fault (Figure 2) reached a peak shortly after 20 Ma [119], which would correspond to a phase of surface unloading in the orogen. We do not see a corresponding subsidence signal in the Swiss Molasse basin. Finally, also in the Swiss part of the Alps/Molasse basin ensemble, the rise of the Alpine topography, and thus the construction of topographic loads occurred at possibly the highest rates between c. 30 and 25 Ma (Figure 7B) [26], but a corresponding flexural pulse is not observed in the basin axis (Figure 9B).

The situation, however, is different in the French portion of the Molasse basin because this basin was situated in a piggy-back position particularly after 20 Ma, and the pulse of rapid subsidence coincides with a period of accelerated crustal uplift and exhumation in the external massifs [120,121]. Therefore, a surface load control on the high sediment accumulation rate in the basin cannot be excluded. Furthermore, the piggy-back emplacement of the French part of the Molasse basin might have influenced the sedimentation pattern, which could introduce a bias upon reconstructing the subsidence history. However, in this part of the Molasse trough, the basin evolution was characterized by a change from a basin-marginal position prior to 20 Ma to an open seaway thereafter, which resulted in the establishment of a connection between the Swiss and the French part of the foreland basin as far South as the Gulf of Lion (GL on Figure 2) [122,123]. Therefore, it is very likely that this subsidence pulse was a regional and not a local signal. Furthermore, the establishment of a seaway along the Alpine front also suggests that the uplift due to the piggy-back emplacement of the basin was not significantly overprinting the inferred regional subsidence signal, which we relate to the tectonic processes in the evolving Alps. In contrast to previous interpretations [21,120,121,123,124], however, we rather consider a slab load control on the c. 20 Ma increase in the subsidence rates than a surface control such as the uplift of the Belledonne external massif (Figure 2). We use the analogy offered by the Aar massif (Figure 2) as an argument because the uplift of this unit was considered to have occurred 'en bloc' through vertical extrusion, possibly driven by buoyancy forces and not by classical thrust tectonics [38,125]. En bloc extrusion of the Aar massif was interpreted to have occurred as an isostatic response to ongoing slab rollback subduction [33,125]. Therefore, such a mechanism would not contribute to the formation of additional surface loads [26]. Accordingly, if such processes [33,38,125] could also be invoked to explain the uplift of the Belledonne massif (Figure 2), then slab loads generated through rollback subduction rather than surface loads would have been the primary control for the formation of accommodation space in the French part of the Molasse basin.

We note that for the Swiss and German Molasse, previous authors, e.g., [6,19,82] explained the formation of the Burdigalian unconformity at 20 Ma through a short period of uplift in the forebulge area. According to these authors, this uplift occurred either as a flexural response to a phase of surface loading in the Alps [6] or as a visco-elastic relaxation of the foreland plate after a phase of thrusting and loading [82]. As outlined above, we refrain from such interpretations because of a lack of evidence in the reconstructed subsidence histories (Figure 9).

In summary, because there is a disconnection between the long-term subsidence pattern in the basin axis and the history of uplift in the Alpine orogen particularly in the area surrounding the Aar massif and the Tauern window, we do not consider that surface loading exerted a major control on the subsidence history of the Molasse basin. Admittedly the situation is different in the Western Alps [21,120,121,123,124] where the hypothesis of a surface load control on the deflection of the foreland plate cannot be completely excluded with the available information.

5.2. Possible Controls of Eustatic Sea-Level Changes on the Development of the Molasse Basin

During most of the time, the Molasse basin had a link to the global sea either via the Paratethys in the NE or the Tethys in the SW [126,127]. This is also the reason why eustatic sea level changes were considered to have controlled the occurrence of transgressions and regressions in the foreland trough [21,68,81,82,92,112,113] and the formation of erosional unconformities, particularly in the Swiss and German parts of the Molasse basin (Figure 6). Such interpretations were justified by the temporal coincidence between the low stands of the eustatic sea level and the occurrence of hiati in the stratigraphic record (e.g., [81,82]). For the Swiss part of the Molasse basin, an eustatic control could even be invoked to explain the erosional unconformities at c. 25 and 22–21 Ma when terrestrial conditions prevailed (Figure 6). We justify this interpretation because the downstream distance to the shoreline (near Munich during USM times) was short enough for sea level to have controlled the elevation of the fluvial base level farther upstream in the Swiss Molasse. Additionally, the unconformities in the Swiss Molasse basin were also formed contemporaneously with those in the German part of the basin when the global sea level was lowered. For the French segment of the basin, however, eustatic sea level changes alone are not sufficient to explain most of the unconformities because the basin was in a piggy-back position where thrusting and uplift beneath the depocenters could have induced the formation of unconformities [21]. Accordingly, while eustatic changes can be invoked to explain the various unconformities identified in the basin axis particularly in the Swiss and German parts of the Molasse basin, the amplitudes of sea level oscillations were most likely too small to explain the large-scale pattern at which accommodation space was formed.

5.3. Slab Load Controls

As outlined above, surface loads and loads due to the basin fill (Figure 1) alone are not capable to explain the large-scale sedimentation pattern in the Molasse basin. As a consequence, we do not consider that upper crustal shortening and the resulting stacking of crustal material (e.g., the uplift of the Aar massif and the buildup of the antiformal stack exposed in the Tauern window, see previous section) had a measurable impact on the basin-scale subsidence pattern of the foreland trough. Instead, we interpret that rollback subduction was the primary mechanism to drive the formation of accommodation space in the basin [33]. As discussed in Kissling and Schlunegger [33], such a model, which has been referred to as rollback orogeny [33,128], differs from considerations where horizontal compression drives the orogenic development of mountain belts. In particular, in an orogen that evolves in response to a rollback subduction, the kinematic processes are mainly driven by the vertically directed slab loads of the subducting plate and not by the horizontal push of the overriding plate [33,128]. Conventionally, the Adriatic plate has been assigned to take this role of exerting a horizontal push. Such a mechanism at work has been proposed in modelling studies that are based on critical taper wedge theories [119,129],

or in scientific contributions that aimed at reconstructing the kinematic evolution of the Alpine orogen [34]. In both cases, a rigid indenter made up of lower crustal material of Adriatic origin has been used either as backstop upon applying critical taper wedge models, or as driver to explain the shortening and uplift in the core of the Alps. However, the results of such analyses cannot be reconciled with two principal observations derived from geophysical surveys [33]. These are first, the strongly negative Bouguer anomalies in the area surrounding the Central Alps [44,46] that could not be explained upon applying critical taper wedge models, and second the occurrence of a kilometre-thick crustal root made up of lower crustal material of the European plate instead of a rigid indenter of Adriatic origin beneath the core of the Alps [45] (Figure 3). Furthermore, as outlined before [33], reconstructions of the evolution of the Alps need to consider the principle where slab loads and topographic loads together with the buoyancy of the crustal root are in an isostatic equilibrium (Figure 1). Accordingly, we take the view where a combination of vertically directed slab loads exerted by the subducted plate (which was only partly counterbalanced by the effects related to the flexural strength of the plate, Figure 1) and the buoyancy of the crustal root were the primary forces to drive the large-scale evolution of the Alps, the formation of accommodation space in the basin and the buildup of topography in the adjacent orogen. In the next sections, we elaborate a scenario of such a dynamic development, and we outline how changes in slab loads offer a valuable alternative for relating the development in the Alps to the sedimentary processes in the foreland basin and the source-to-sink routing in this sedimentary trough.

5.3.1. Prior to 32 Ma: Flysch Stage in the Entire Molasse Basin

The start of the Molasse basin as a foreland basin involved a Flysch stage and was characterized by a deep-marine trough next to the Alpine thrust front (Figure 8A). During these times, the formation of a deep trough appears to have been controlled by the downward-directed slab loads exerted by the subducted oceanic lithosphere slab of the European plate, which resulted in the downwarping of the foreland plate (Figure 11A,B). Beneath the Central and Western Alps, this downwarping was most likely less than beneath the Eastern Alps. This interpretation is based on the eastward-directed routing of the clastic material in the submarine system (Figure 8A), which points towards an eastward-directed tilt of the foreland plate and thus towards a greater deflection of the foreland plate in the East. The along-strike difference in the deflection of the basin trough most likely reflects the effect of the buoyancy caused by the crustal material of the Iberian plate, which was, prior to 35 Ma, accreted to the orogen in its central and western part but not in its eastern portion (Figure 7). As a further consequence of this buoyancy, the incipient Alpine topography was possibly higher in the Western and Central Alps than in the Eastern Alps. These along-strike differences in the topography possibly explain why sediment budgets disclosed a 50% higher sediment yield in the Western and Central Alps compared to the eastern part of the orogen [130,131].

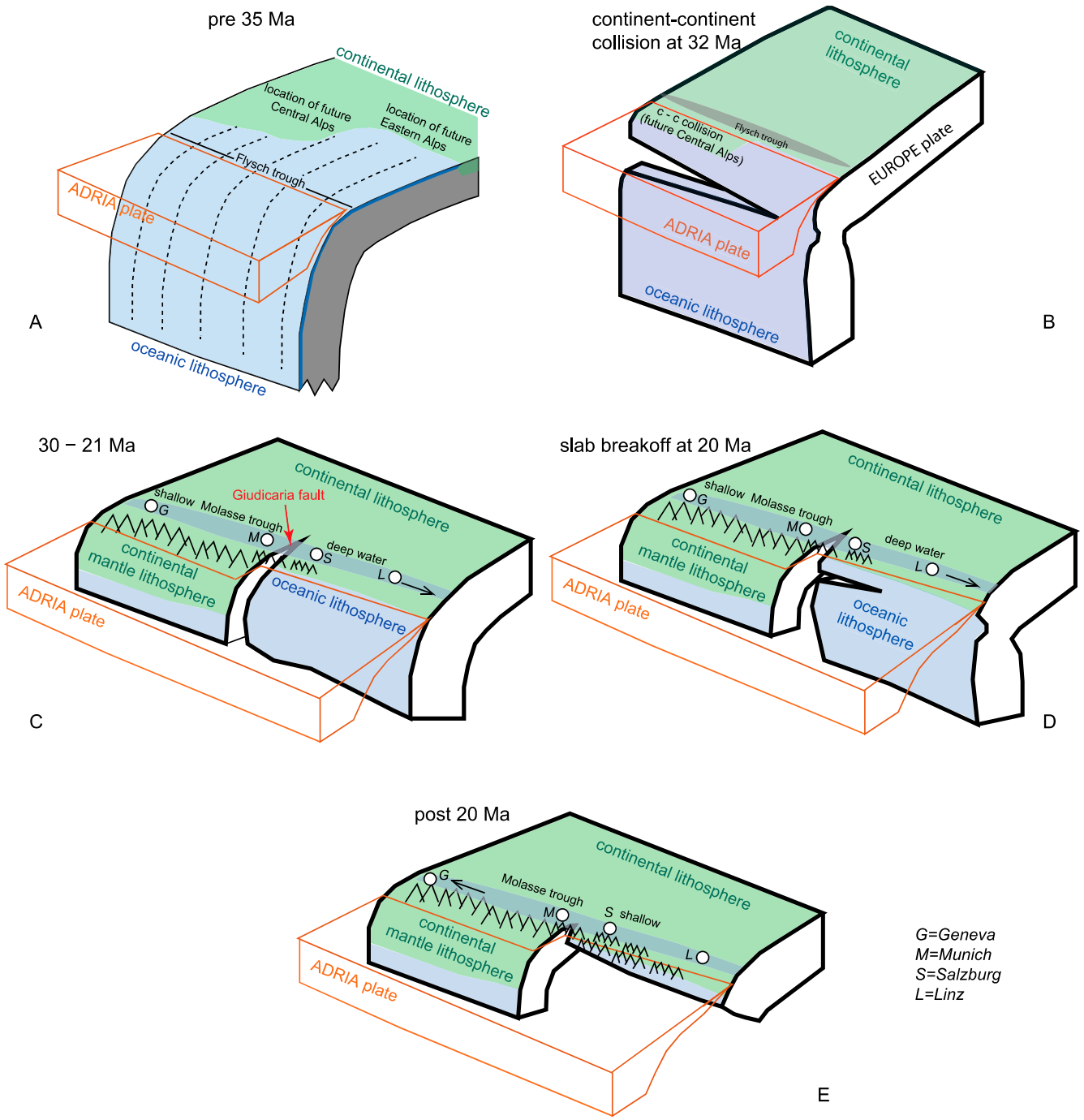

Figure 11. Sketch figure, showing the development of the collisional processes and the basin response. (**A**) Situation before 35 Ma, when the European oceanic plate was subducting beneath the Adriatic plate and when a flysch trough was established. (**B**) At c. 32 Ma, continent-continent collision started beneath the Central Alps. This resulted in necking and the removal of the subducted oceanic plate. (**C**) Slab breakoff beneath the Central Alps was associated with a rebound of the foreland plate and the growth of the Central Alpine topography. As a result, the erosional mass flux increased in the Central Alps, and the Molasse basin transitioned from the underfilled Flysch to the overfilled Molasse stage. Beneath the Eastern Alps, parts of the subducted oceanic plate remained attached to the continental plate, which resulted in a continued downwarping of the foreland plate. Therefore, the topography of the Eastern Alps was subdued, and the foreland basin remained in the Flysch stage. (**D**) Incipient slab

delamination beneath the Eastern Alps resulted in a rebound of the foreland plate, with the consequence that the Eastern Molasse basin transitioned from deep marine to shallow marine conditions. The rise of the Eastern Alpine topography was less than in the Central Alps at 30 Ma, mainly because the buoyant crustal root was much thinner in the East. (**E**) Subduction of the continental lithosphere continued beneath the Central Alps after 20 Ma, which resulted in an ongoing downwarping of the foreland plate. This finally resulted in a reversal of the drainage direction.

5.3.2. At 30 Ma: Slab Load Controls on the Along-Strike Differences in Sedimentation

At 32 Ma, after the collision between the continental plates, crustal rocks of the European continental plate together with the accreted material of the Iberian plate started to enter the subduction channel (Figure 7). Partly due to the buoyancy of the continental crust, the continental lithosphere has a higher effective flexural rigidity than the subducted oceanic lithosphere. The result was an increase in the extensional forces at the interface between the continental and oceanic parts of the European plate, with the consequence that eventually the subducted oceanic lithosphere slab broke off. The continental part of the plate, in turn, experienced a rebound because of the removal of the downward-directed slab weight and because of the buoyancy of the crustal root (Figure 7B) [33]. The related uplift was accomplished by backthrusting along the Periadriatic lineament. It resulted in the rise of the Alpine topography and in an increase in the sediment yields from <5000 km^3/My to >20,000 km^3/My [130,131]. We use the combination of these processes to explain the transition of the Molasse basin from the underfilled Flysch to the overfilled Molasse stage particularly between Chambery and Munich [105] (Figure 8). Accordingly, this shift from basin underfill to overfill is interpreted as a combined response to the rebound of the foreland plate and to the buoyancy exerted by the accreted crustal root.

Please note, however, that the 30 Ma-old slab break-off hypothesis was contested [132] based on evidence for the occurrence of magmatism along the Periadriatic lineament when subduction was still active, and because zircon U–Pb data [132] reveal a trend towards younger ages perpendicular to the strike-direction of the European slab. This information was then used to propose that the European slab was continuously steepening between the Eocene–Oligocene without breaking off [132]. However, this interpretation is not consistent with the development of the Molasse basin, mainly because slab steepening would be associated with a period of continued Flysch sedimentation and not with a shift from basin underfill to overfill.

In the Eastern Alps, at least a part of the oceanic slab most likely remained attached to the European plate, thereby causing a downward-directed flexure of this plate and maintaining the Flysch stage (Figure 11C). In the basin axis, the increasing subsidence rate particularly after 25 Ma together with the rapid northward shift of the orogen front (Figure 9C) and onlaps of the Puchkirchen and Zupfing Formations on what has been referred to as the Northern Slope Unconformity [19] suggest that the rollback subduction of the oceanic part of the European plate was ongoing, driven by its own load (Figure 7G). Furthermore, because no large volume of crustal material was accreted to form a buoyant crustal root, the topography of the Eastern Alps was most likely lower than in the Western and Central Alps (Figure 11C). This could explain why the sediment yields were >50% lower than in the Western and Central Alps. In fact, provenance tracing revealed that most of the detritus in the Puchkirchen Formation (Figure 8B) was sourced from the eastern margin of the Central Alps surrounding the Periadratic lineament [20] and thus not from the Eastern Alps. Please note that in this context we consider the boundary between the Central and Eastern Alps to be situated in the area of the Giudicaria fault (Figure 2). Because of the rapid rollback deflection of the foreland plate, accommodation space was not only formed in the basin axis but also on top of the frontal part of the eastern Alpine wedge. There a >1000 m-thick suite of fluvio-deltaic material derived from the Eastern Alps [20] accumulated in a wedge-top position (Augenstein Formation, Figure 8B). Accordingly, between 30 and 20 Ma, the along-strike difference in the deflection of the foreland plate and the sediment routing pattern most likely reflects the response to the

larger slab loads beneath the Eastern Alps (Figure 11C). In fact, the yet still attached oceanic lithosphere was likely to have exerted a larger vertical-directed slab load than the more rigid subducted lithospheric mantle slab of the European plate beneath the Central Alps (Figure 11C), thereby tilting the foreland plate to the East. If this interpretation is valid, then the development of the marginal facies in the western Molasse basin [110] could reflect the occurrence of a lateral forebulge that established in response to the eastward, arcuate-shaped deflection of the European plate.

Note that between 30–25 Ma, the reconstructed subsidence rate of the Austrian Molasse was significantly lower than in the German part of the basin (Figures 9 and 10), which could be perceived as not consistent with the scenario drawn in this section. We interpret this pattern by the differences in the distance between the Alpine front and the sites for which we calculated the subsidence history. Because prior to 25 Ma, the Austrian section was situated farther away from the orogen front (c. 160 km) than the German section (c. 100 km, Figure 8A), the subsidence rates were lower at the Austrian site. The situation then changed during the time between 25 and 20 Ma, when ongoing rollback subduction and the associated propagation of the orogenic front shifted the Austrian section as close to the orogen front as the German one (Figure 8B). It thus appears that the propagation rate of the Alpine front (and the rollback subduction rate) was higher in the Austrian (i.e., east of the northward extension of the Giudicaria fault) than in the German part (west of the northward extension of this fault, Figure 11), which offers an explanation as to why the subsidence rates accelerated more rapidly in the Austrian Molasse basin.

5.3.3. At 20 Ma: Controls of Slab Unloading Beneath the Eastern Alps

The situation then changed at c. 20 Ma, when the subducted oceanic part of the European plate broke off beneath the Eastern Alps (Figure 11D,E). The result of this slab unloading was a rebound of the eastern segment of the foreland plate (Figure 7H), while the lithospheric mantle slab remained attached to the European plate in its central and western segments and continued to be subducted. This rebound, however, was possibly less than in the Central Alps at 30 Ma, because beneath the Eastern Alps, a smaller volume of continental crust was delaminated from its mantle lithosphere prior to slab breakoff than beneath the Central Alps. Therefore, less continental crust was accumulated to establish a buoyant crustal root beneath the eastern part of the orogen to counterbalance the slab loads and to maintain a moderately high topography. The removed slab was most likely replaced by the lithospheric mantle slab of the Adriatic plate (Figure 7I). As a result, the Po Basin on the eastern side of the Giudicaria fault became the active foreland basin where subsidence rates started to increase (Figure 12).

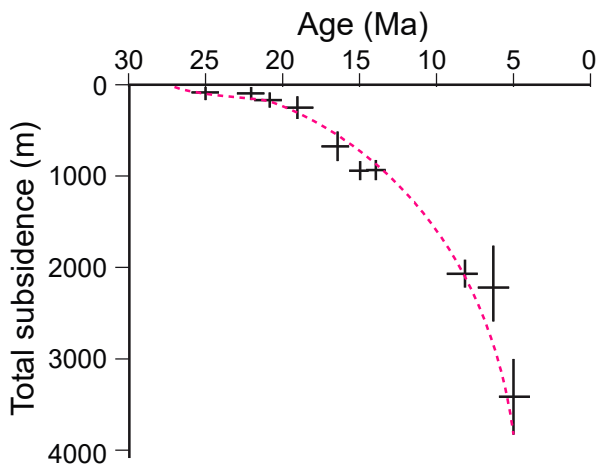

Figure 12. Evolution of the total subsidence of the Po basin recorded by sections that are exposed in the hangingwall of the Montello thrust (see site labelled with 'P' in Figure 2 for location). The subsidence pattern [133] has been corrected for eustatic sea level variations and compaction.

The plate underneath the eastern Molasse experienced a phase of unloading at 20 Ma, while ongoing subduction resulted in a further downwarping of the foreland plate beneath the central and western Molasse basin (Figure 11D,E). These along-strike differences are mirrored in the along-strike pattern of the basin's subsidence rates. In the eastern part, the subsidence rates of the foreland plate decreased to <50 m/My at 20 Ma, whereas the subsidence rates continued to increase to ca. 400–500 m/My in the central part of the basin, and to nearly 1000 m/My in its western segment (Figure 9). These differences are also recorded in the facies development. In the eastern part of the basin, the facies shifted from a Flysch-type environment to shallow marine conditions at 20 Ma analogously to what occurred around 30 Ma in the western part of the basin. This change is recorded by the N-directed clinoforms of the Hall Formation [19] and onlap structures of this unit on top of the Puchkirchen Formation, thereby forming the Base Hall Unconformity [19]. We consider these processes as response to the rebound of the foreland plate and the larger fluxes of sediment derived from the rising Eastern Alps. However, the largest portion of this material was derived through the recycling of the previously deposited Augenstein unit [20], which became uplifted possibly in response to this rebound.

In the central and western part of the Molasse basin, the ongoing increase in the subsidence rates after 20 Ma (Figure 9) in combination with a 30% reduction in sediment flux [130,131] and possibly a rise in the eustatic sea level [81,82,112,113,134] caused the fluvial depocenters to step back, thereby giving way to a marine environment. Near Lucerne (Figure 2), the first transgression progressed from the East to the West at 20 Ma, whereas the subsequent transgression at 18 Ma occurred in the opposition direction [17,112]. This suggests that between 20 and 18 Ma, the tilt of the basin axis reversed from an east- to a west-directed orientation (Figure 10C). This reversal is thus considered as a direct response to the foreland plate to slab unloading beneath the Eastern Alps, while subduction of the lithospheric mantle slab beneath the Central and Western Alps proceeded (Figure 11), which ultimately resulted in westward tilt of the foreland plate.

6. Conclusions

We propose a qualitative geodynamic model where subduction tectonics beneath the Alps has controlled the large-scale evolution of the Molasse foreland basin. In particular, based on a synthesis of published data, we document that at 30 Ma, the change from the deep marine underfilled (Flysch stage) to the overfilled terrestrial Molasse stage of basin evolution was most likely driven by slab unloading beneath the Western and Central Alps. This is considered to have resulted in a growth of the Alpine topography in this part of the Alps, an increase in surface erosion and sediment supply to the basin, and thus in the observed change from basin underfill to overfill. In the eastern part of the basin, however, the underfilled Flysch-type conditions prevailed until 20 Ma, which we relate to the occurrence of slab loads beneath the Eastern Alps as parts of the subducted oceanic slab most likely remained attached to the European plate and downwarped the plate in the East. The situation changed at 20 Ma, when the eastern part of the basin experienced a change from deep marine underfilled to shallow marine filled and finally overfilled conditions. This was also the time when the sediment routing in the basin axis changed from an east-directed sediment dispersal prior to 20 Ma, to a west-oriented sediment transport and thus to the opposite direction thereafter. We relate these changes to the occurrence of oceanic slab breakoff beneath the Eastern Alps, which most likely resulted in a rebound of the plate, a growth of the topography in these parts of the Alps and a larger sediment flux to the eastern portion of the basin. We thus propose that there is ample evidence in the basin-scale stratigraphic record for a slab load control on the development of the Molasse foreland basin.

In a broader sense, we suggest that the combination of slab loads and the buoyancy of the crustal root beneath an orogen are likely to exert a control on the formation of accommodation space in a foreland basin and the routing of sediment in this trough. These loads and forces also impact the formation of relief and the topography in the orogen. They

additionally control the production of sediment where a higher topography, conditioned by the buoyancy of a crustal root, can result in higher denudation rates and thus in a larger material supply to the adjacent foreland basin. Finally, the formation of such a crustal root and the accretion of crustal material is ultimately controlled by slab rollback subduction, which in turn is driven by slab loads. Consequently, any changes in the arrangement of these forces, such as slab tearing and slab breakoff, has the potential to alter the production rates of sediment in the orogen, the formation rate of accommodation space in the basin and the dispersion of the sedimentary material from source to sink. Such changes are ultimately recorded by the sedimentary archives in a foreland basin. We propose that the Alps/Molasse basin ensemble serve as presumably one of the best examples where such mechanisms at work can be documented, and we suggest that further research on the relationships between subduction tectonics, orogenesis and foreland basin evolution will significantly enhance our understanding of how a foreland basin in general responds to orogenic processes at deeper crustal levels.

Author Contributions: This study was designed by both authors. F.S. wrote the text with contributions by E.K. Both authors drafted the figures and contributed to the discussion. All authors have read and agreed to the published version of the manuscript.

Funding: This research received funding from the University of Bern.

Institutional Review Board Statement: Not applicable.

Informed Consent Statement: Not applicable.

Data Availability Statement: All data that has been used for this contribution is presented in this article, or the references to the data sources are given.

Acknowledgments: We kindly acknowledge the editors for handling this manuscript and three anonymous reviewers for their constructive comments.

Conflicts of Interest: The authors declare no conflict of interest.

References

1. DeCelles, P.; Giles, K.A. Foreland basin systems. *Basin Res.* **1996**, *8*, 105–123. [CrossRef]
2. DeCelles, P.G.; Gehrels, G.E.; Quade, J.; Ojha, T.P. Eocene-early Miocene foreland basin development and the history of Himalayan thrustiing, western and central Nepal. *Tectonics* **1998**, *5*, 741–765. [CrossRef]
3. Garcia-Castellanos, D.; Fernàndez, M.; Torne, M. Modeling the evolution of the Guadalquivir foreland basin (southern Spain). *Tectonics* **2002**, *21*, 1018. [CrossRef]
4. Sinclair, H.D.; Naylor, M. Foreland basin subsidence driven by topographic growth versus plate subduction. *Geol. Soc. Amer. Bull.* **2012**, *124*, 368–379. [CrossRef]
5. Horton, B.K. Sedimentary record of Andean mountain building. *Earth-Sci. Rev.* **2018**, *178*, 279–309. [CrossRef]
6. Sinclair, H.D.; Coakley, B.J.; Allen, P.A.; Watts, A.B. Simulation of foreland basin stratigraphy using a diffusion model of mountain belt uplift and erosion: An example from the Central Alps, Switzerland. *Tectonics* **1991**, *10*, 599–620. [CrossRef]
7. Flemings, P.B.; Jordan, T.E. Stratigraphic modeling of foreland basins: Interpreting thrust deformation and lithosphere rheology. *Geology* **1990**, *18*, 430–434. [CrossRef]
8. Jordan, T.E.; Flemings, P.B. Large-scale stratigraphic architecture, eustatic variation, and unsteady tectonism: A theoretical evaluation. *J. Geophys. Res.-Solid Earth* **1991**, *96*, 6681–6699. [CrossRef]
9. Turcotte, D.L.; Schubert, G. *Geodynamics: Application of Continuum Physics to Geological Problems*; John Wiley: New York, NY, USA, 1982; p. 650.
10. Jordan, T.E. Thrust loads and foreland basin evolution, Cretaceous, western United States. *AAPG Bull.* **1981**, *65*, 2506–2520.
11. Beaumont, C. Foreland basins. *Geophys. J. Int.* **1981**, *65*, 291–329. [CrossRef]
12. Füchtbauer, H. Sedimentpetrographische Untersuchungen in der älteren Molasse nördlich der Alpen. *Eclogae Geol. Helv.* **1964**, *61*, 157–298.
13. Pfiffner, O.A. Evolution of the north Alpine foreland basin in the Central Alps. In *Foreland Basins*; Allen, P.A., Homewood, P., Eds.; John Wiley & Sons: New York, NY, USA, 1986; Volume 8, pp. 219–228.
14. Schlunegger, F.; Matter, A.; Burbank, D.W.; Klaper, E.M. Magnetostratigraphic constraints on relationships between evolution of the central Swiss Molass Basin and Alpine orogenic events. *Geol. Soc. Am. Bull.* **1997**, *109*, 225–241. [CrossRef]
15. Zweigel, J. Eustatic versus tectonic control on foreland basin fill: Sequences stratigraphy, subsidence analysis, stratigraphic modeling, and reservoir modeling applied to the German Molasse basin. *Contr. Sed. Geol.* **1998**, *20*, 140.

16. Kempf, O.; Matter, A.; Burbank, D.W.; Mange, M. Depositional and structural evolution of a foreland basin margin in a magnetostratigraphic framework; the eastern Swiss Molasse Basin. *Int. J. Earth Sci.* **1999**, *88*, 253–275. [CrossRef]
17. Strunck, P.; Matter, A. Depositional evolution of the western Swiss Molasse. *Eclogae Geol. Helv.* **2002**, *95*, 197–222.
18. Sinclair, H.D.; Allen, P.A. Vertical versus horizontal motions in the Alpine orogenic wedge: Stratigraphic response in the foreland basin. *Basin Res.* **1992**, *4*, 215–232. [CrossRef]
19. Hülscher, J.; Fischer, G.; Grunert, P.; Auer, G.; Bernhardt, A. Selective recording of the tectonic forcings in an Oligocene/Miocene submarine channel system: Insights from new age constraints and sediment volumes from the Austrian northern Alpine foreland basin. *Front. Earth Sci.* **2019**, *7*, 302. [CrossRef]
20. Hülscher, J.; Sobel, E.R.; Verwater, V.; Groß, P.; Chew, D.; Bernhardt, A. Detrital apatite geochemistry and thermochronology from the Oligocene/Miocene Alpine foreland record the early exhumation of the Tauern Window. *Basin Res.* **2021**, *33*, 3021–3044. [CrossRef]
21. Kalifi, A.; Leloup, P.H.; Sorrel, P.; Galy, A.; Demory, F.; Spina, V.; Huet, B.; Quillévéré, F.; Ricciardi, F.; Michoux, D.; et al. Chronology of thrust propagation from an updated tectono-sedimentary framework of the Miocene molasse (western Alps). *Solid Earth* **2021**, *12*, 2735–2771. [CrossRef]
22. Rögl, F.; Hochuli, P.; Müller, C. Oligocene-early miocene stratigraphic correlations in the molasse basin of Austria. *Ann. Geol. Pay. Hell. Tome Hors Series* **1979**, *30*, 1045–1050.
23. Spiegel, C.; Kuhlemann, J.; Dunkl, I.; Frisch, W.; von Eynatten, H.; Balogh, K. The erosion history of the Central Alps: Evidence from zircon fission track data of the foreland basin sediments. *Terra Nova* **2000**, *12*, 163–170. [CrossRef]
24. Anfinsion, O.A.; Stockli, D.F.; Miller, J.C.; Möller, A.; Schlunegger, F. Tectonic exhumation of the Central Alps recorded by detrital zircon in the Molasse Basin, Switzerland. *Solid Earth* **2020**, *11*, 2197–2220. [CrossRef]
25. Pfiffner, O.A.; Schlunegger, F.; Buiter, S.J.H. The Swiss Alps and their peripheral foreland basin: Stratigraphic response to deep crustal processes. *Tectonics* **2002**, *6*, 1054. [CrossRef]
26. Schlunegger, F.; Kissling, E. Slab rollback orogeny in the Alps and evolution of the Swiss Molasse basin. *Nat. Commun.* **2015**, *6*, 8605. [CrossRef] [PubMed]
27. Kuhlemann, J. Paleogeographic and paleotopographic evolution of the Swiss and Eastern Alps since the Oligocene. *Glob. Planet. Chang.* **2007**, *58*, 224–236. [CrossRef]
28. Handy, M.R.; Schmid, S.M.; Paffrath, M.; Friederich, W.; the AlpArray Working Group. Orogenic lithosphere and slabs in the greater Alpine area–interpretations based on teleseismic P-wave tomography. *Solid Earth* **2021**, *12*, 2633–2669. [CrossRef]
29. Lippitsch, R.; Kissling, E.; Ansorge, J. Upper mantle structure beneath the Alpine orogen from high-resolution teleseismic tomography. *J. Geophys. Res.* **2003**, *108*, 2376. [CrossRef]
30. Froitzheim, N.; Schmid, S.M.; Frey, M. Mesozoic paleogeography and the timing of eclogite-facies metamorphism in the Alps: A working hypothesis. *Eclogae Geol. Helv.* **1996**, *89*, 81–110.
31. Schmid, S.M.; Fügenschuh, B.; Kissling, E.; Schuster, R. Tectonic map and overall architecture of the Alpine orogen. *Eclogae Geol. Helv.* **2004**, *97*, 93–117. [CrossRef]
32. Handy, M.; Schmid, S.; Bousquet, R.; Kissling, E.; Bernoulli, D. Reconciling plate-tectonic reconstructions of Alpine Tethys with the geological-geophysical record of spreading and subduction in the Alps. *Earth-Sci. Rev.* **2010**, *102*, 121–158. [CrossRef]
33. Kissling, E.; Schlunegger, F. Rollback orogeny model for the evolution of the Swiss Alps. *Tectonics* **2008**, *37*, 1097–1115. [CrossRef]
34. Schmid, S.M.; Pfiffner, O.A.; Froitzheim, N.; Schönborn, G.; Kissling, E. Geophysical-geological transect and tectonic evolution of the Swiss-Italian Alps. *Tectonics* **1996**, *15*, 1036–1064. [CrossRef]
35. Rosenberg, C.L.; Berger, A.; Bellahsen, N.; Bousquet, R. Relating orogen width to shortening, erosion, and exhumation during Alpine collision. *Tectonics* **2015**, *34*, 1306–1328. [CrossRef]
36. Rosenberg, C.L.; Schneider, S.; Scharf, A.; Bertrand, A.; Hammerschmidt, K.; Rabaute, A.; Brun, J.-P. Relating collisional kinematics to exhumation processes in the Eastern Alps. *Earth-Sci. Rev.* **2018**, *176*, 311–344. [CrossRef]
37. Handy, M.R.; Ustaszewski, K.; Kissling, E. Reconstructing the Alps-Carpathians-Dinarides as key to understanding switches in subduction polarity, slab gaps and surface motion. *Int. J. Earth Sci.* **2015**, *104*, 1–26. [CrossRef]
38. Herwegh, M.; Berger, A.; Glotzbach, C.; Wangenheim, C.; Mock, S.; Wehrens, P.; Baumberger, R.; Egli, D.; Kissling, E. Late stages of continent-continent collision: Timing, kinematic evolution, and exhumation of the Northern rim (Aar Massif) of the Alps. *Earth-Sci. Rev.* **2020**, *200*, 102959. [CrossRef]
39. Schönborn, G. Alpine tectonics and kinematic models of the Central Southern Alps. *Mem. Soc. Geol.* **1992**, *44*, 229–393.
40. Ustaszewski, K.; Schmid, S.M.; Fügenschuh, B.; Tischler, M.; Kissling, E.; Spakman, W. A map-view restoration of the Alpine-Carpathian-Dinaridic system for the Early Miocene. *Swiss J. Geosci.* **2008**, *101*, 273–294. [CrossRef]
41. Stipp, M.; Fügenschuh, B.; Gromet, L.P.; Stünitz, H.; Schmid, S.M. Contemporaneous plutonism and strike-slip faulting: A case study from the Tonale fault zone north of the Adamello pluton (Italian Alps). *Tectonics* **2004**, *23*, TC3004. [CrossRef]
42. Ratschbacher, L.; Frisch, W.; Linzer, H.G.; Merle, O. Lateral extrusion in the Eastern Alps, part 2: Structural analysis. *Tectonics* **1991**, *10*, 257–271. [CrossRef]
43. Frisch, W.; Dunkl, I.; Kuhlemann, J. Post-collisional orogen-parallel large-scale extension in the Eastern Alps. *Tectonophysics* **2000**, *327*, 239–265. [CrossRef]
44. Kissling, E.; Schmid, S.; Lippitsch, R.; Ansorge, J.; Fügenschuh, B. Lithosphere structure and tectonic evolution of the Alpine arc: New evidence from high-resolution teleseismic tomography. *Geol. Soc. London Mem.* **2006**, *32*, 129–145. [CrossRef]

45. Fry, B.; Deschamps, F.; Kissling, E.; Stehly, L.; Giardini, D. Layered azimuthal anisotropy of Rayleigh wave phase velocities in the European Alpine lithosphere inferred from ambient noise. *Earth Planet. Sci. Lett.* **2010**, *297*, 95–102. [CrossRef]
46. Lyon-Caen, H.; Molnar, P. Constraints on the deep structure and dynamic processes beneath the Alps and adjacent regions from an analysis of gravity anomalies. *Geophys. J. Int.* **1998**, *99*, 19–32. [CrossRef]
47. Holliger, K.; Kissling, E. Gravity interpretation of a unified 2-D acoustic image of the central Alpine collision zone. *Geophys. J. Int.* **1992**, *111*, 213–225. [CrossRef]
48. Zhao, L.; Paul, A.; Malusà, M.G.; Xu, X.; Zheng, T.; Solarino, S.; Guillot, S.; Schwartz, S.; Dumont, T.; Salimbeni, S.; et al. Continuity of the Alpine slab unraveled by high-resolution P wave tomography. *J. Geophys. Res.-Solid Earth* **2016**, *121*, 8720–8737. [CrossRef]
49. Beller, S.; Monteiller, V.; Operto, S.; Nolet, G.; Paul, A.; Zhao, L. Lithospheric architecture of the South-Western Alps revealed by multiparameter teleseismic full-waveform inversion. *Geophys. J. Int.* **2018**, *212*, 1369–1388. [CrossRef]
50. Lammerer, H.; Gebrande, E.; Lüschen, E.; Veselá, P. A crustal-scale cross-section through the Tauern Window (eastern Alps) from geophysical and geological data. *Geol. Soc. London Spec. Publ.* **2008**, *298*, 219–229. [CrossRef]
51. Scharf, A.; Handy, M.R.; Favaro, S.; Schmid, S.M.; Bertrand, A. Modes of orogen-parallel stretching and extensional exhumation in response to microplate indentation and roll-back subduction (Tauern Window, Eastern Alps). *Int. J. Earth Sci.* **2013**, *102*, 1627–1654. [CrossRef]
52. Kaestle, E.D.; Rosenberg, C.; Boschi, L.; Bellahsen, N.; Meier, T.; El-Sharkawy, A. Slab break-offs in the Alpine subduction zones. *Int. J. Earth Sci.* **2020**, *109*, 587–603. [CrossRef]
53. Piromallo, C.; Morelli, A. P-wave tomography of the mantle under the Alpine–Mediterranean area. *J Geophys. Res.* **2003**, *108*, 2065. [CrossRef]
54. Karousova, H.; Plomerova, J.; Babuska, V. Upper-mantle structure beneath the southern Bohemian Massif and its surroundings imaged by high-resolution tomography. *Geophys. J. Int.* **2013**, *194*, 1203–1215. [CrossRef]
55. Dando, B.D.E.; Stuart, G.W.; Houseman, G.A.; Hegedüs, E.; Brückl, E.; Radovanović, S. Teleseismic tomography of the mantle in the Carpathian–Pannonian region of central Europe. *Geophys. J. Int.* **2011**, *186*, 11–31. [CrossRef]
56. Mitterbauer, U.; Behm, M.; Brückl, E.; Lippitsch, R.; Guterch, A.; Keller, G.R.; Koslovskaya, E.; Rumpfhuber, E.M.; Sumanovac, F. Shape and origin of the East-Alp slab constrained by the ALPASS teleseismic model. *Tectonophysics* **2011**, *510*, 195–206. [CrossRef]
57. Wortel, M.J.R.; Spakman, W. Subduction and slab detachment in the Mediterranean-Carpathian region. *Science* **2000**, *290*, 1910–1917. [CrossRef]
58. Spakman, W.; Wortel, M.J.R. Tomographic View on Western Mediterranean Geodynamics. In *The TRANSMED Atlas, the Mediterranean Region from Crust to Mantle*; Cavazza, W., Roure, F.M., Stampfli, G.M., Ziegler, P.A., Eds.; Springer: Berlin/Heidelberg, Germany, 2004; pp. 31–52. [CrossRef]
59. Linzer, H.-G.; Decker, K.; Peresson, H.; Dell'Mour, R.; Frisch, W. Balancing lateral orogenic float of the Eastern Alps. *Tectonophysics* **2002**, *354*, 211–237. [CrossRef]
60. Zahorec, P.; Papčo, J.; Pašteka, R.; Bielik, M.; Bonvalot, S.; Braitenberg, C.; Ebbing, J.; Gabriel, G.; Gosar, A.; Grand, A.; et al. The first pan-Alpine surface-gravity database, a modern compilation that crosses frontiers. *Earth Syst. Sci. Data* **2021**, *13*, 2165–2209. [CrossRef]
61. Spada, M.; Bianchi, I.; Kissling, E.; Agostinetti, N.P.; Wiemer, S. Combining controlled-source seismology and receiver function information to derive 3-D Moho topography for Italy. *Geophys. J. Int.* **2013**, *194*, 1050–1068. [CrossRef]
62. Laubscher, H.P. The arcs of the Western Alps and the Northern Apennines: An updated view. *Tectonophysics* **1998**, *146*, 67–78. [CrossRef]
63. Speranza, F.; Villa, I.M.; Sagnotti, L.; Florindo, F.; Cosentino, D.; Cipollari, P. Age of the Corsica-Sardinia rotation and Liguro-Provençal Basin spreading: New paleomagnetic and Ar/Ar evidence. *Tectonophysics* **2002**, *347*, 231–251. [CrossRef]
64. Argnani, A. Plate motion and the evolution of Alpine Corsica and Northern Apennines. *Tectonophysics* **2012**, *579*, 207–219. [CrossRef]
65. Carminati, E.; Doglioni, C. Alps vs. Apennines: The paradigm of a tectonically asymmetric Earth. *Earth-Sci. Rev.* **2012**, *112*, 67–96. [CrossRef]
66. Amadori, C.; Toscani, G.; Di Giulio, A.; Maesano, F.; D'Ambrogi, C.; Ghielmi, M.; Fantoni, R. From cylindrical to non-cylindrical foreland basin: Pliocene-Pleistocene evolution of the Po Plain-Northern Adriatic Basin (Italy). *Basin Res.* **2019**, *31*, 991–1015. [CrossRef]
67. Sissingh, W. Tectonostratigraphy of the North Alpine Foreland Basin: Correlation of Tertiary depositional cycles and orogenic phases. *Tectonophysics* **1997**, *282*, 223–256. [CrossRef]
68. Sissingh, W. Comparative Tertiary stratigraphy of the Rhine Graben, Bresse Graben and Molasse Basin: Correlation of Alpine foreland events. *Tectonophysics* **1998**, *300*, 249–284. [CrossRef]
69. Berger, J.-P.; Reichenbacher, B.; Becker, D.; Grimm, M.; Grimm, K.; Picot, L.; Storni, A.; Pirkenseer, C.; Derer, C.; Schäfer, A. Paleogeography of the Upper Rhine Graben (URG) and the Swiss Molasse Basin (SMB) from Eocene to Pliocene. *Int. J. Earth Sci.* **2005**, *94*, 697–710. [CrossRef]
70. Burkhard, M. Aspects of the large-scale miocene deformation in the most external part of the Swiss Alps (Sub-Alpine Molasse to Jura Fold Belt). *Eclogae Geol. Helv.* **1990**, *83*, 559–583.
71. Cederbom, C.; Sinclair, H.D.; Schlunegger, F.; Rahn, M. Climate-induced rebound and exhumation of the European Alps. *Geology* **2004**, *32*, 709–712. [CrossRef]

72. Hinsch, R. Laterally varying structure and kinematics of the molasse fold and thrust belt of the central eastern alps: Implications for exploration. *AAPG Bull.* **2013**, *97*, 1805–1831. [CrossRef]
73. Ortner, H.; Aicholzer, S.; Zerlauth, M.; Pilser, R.; Fügenschuh, B. Geometry, amount, and sequence of thrusting in the Subalpine Molasse of western Austria and southern Germany, European Alps. *Tectonics* **2015**, *34*, 1–30. [CrossRef]
74. Malz, A.; Madritsch, H.; Jordan, P.; Meier, B.; Kley, J. Along-strike variation of thin-skinned thrusting style controlled by pre-existing basement structure in the easternmost Jura Mountains (Northern Switzerland). In *Fold and Thrust Belts: Structural Style, Evolution and Exploration*; Hammerstein, J.A., di Cuia, R., Cottam, M.A., Zamora, G., Butler, R.W.H., Eds.; Geological Society of London: London, UK, 2019; Volume 490, pp. 199–220.
75. Sommaruga, A.; Eichenbeger, U.; Marillier, F. *Seismic Atlas of the Swiss Molasse Basin*; Swiss Geophysical Commission, Ed.; Matér. Géol. Suisse, Géophys; 2012; p. 44. Available online: https://www.geologieportal.ch/en/themes/fundamentals-of-geology/geophysics/seismic-atlas.html (accessed on 23 May 2022).
76. Tesauro, M.; Kaban, M.K.; Cloetingh, S.A.P.L. A new thermal and rheological model of the European lithosphere. *Tectonophysics* **2009**, *476*, 478–495. [CrossRef]
77. Mey, J.; Scherler, D.; Wickert, A.D.; Egholm, D.L.; Tesauro, M.; Schildgen, T.F.; Strecker, M. Glacial isostatic uplift of the European Alps. *Nat. Comm.* **2016**, *7*, 13382. [CrossRef] [PubMed]
78. Waschbusch, P.J.; Royden, L.H. Spatial and temporal evolution of foredeep basins: Lateral strength variations and inelastic yielding in continental lithosphere. *Basin Res.* **1992**, *4*, 179–196. [CrossRef]
79. Matter, A.; Homewood, P.; Caron, C.; Rigassi, D.; van Stuijvenberg, J.; Weidmann, M.; Winkler, W. Flysch and Molasse of Western and Central Switzerland. In *Geology of Switzerland Exc. Guidebook No. 126A, Proceedings of the 26th International Geological Congress, Paris, France, 15 January 1980*; Geol. Komm.; Wepf & Co.: Basel, Switzerland, 1980.
80. Kuhlemann, J.; Kempf, O. Post-Eocene evolution of the North Alpine Foreland Basin and its response to Alpine tectonics. *Sediment. Geol.* **2002**, *152*, 45–78. [CrossRef]
81. Jin, J.; Aigner, T.; Luterbacher, H.P.; Bachmann, G.H.; Müller, M. Sequence stratigraphy and depositional history in the south-eastern German Molasse Basin. *Mar. Petrol. Geol.* **1995**, *12*, 929–936. [CrossRef]
82. Zweigel, J.; Aigner, T.; Luterbacher, H. Eustatic versus tectonic controls on Alpine foreland basin fill: Sequence stratigraphy and subsidence analysis in the SE German Molasse. In *Cenzoic Foreland Basins of Western Europe*; Mascle, A., Puigdefabregas, C., Luterbacher, H.P., Fernandez, M., Eds.; Geological Society of London: London, UK, 1998; Volume 134, pp. 299–323.
83. Cederbom, C.; van der Beek, P.; Schlunegger, F.; Sinclair, H.; Oncken, O. Rapid extensive erosion oft he North Alpine foreland basin at 5-4 Ma. *Basin Res.* **2011**, *23*, 528–550. [CrossRef]
84. Baran, R.; Friedrich, A.; Schlunegger, F. The late Miocene to Holocene erosion pattern of the Alpine foreland reflects Eurasian slab unloading beneath the western Alps rather than global climate change. *Lithosphere* **2014**, *6*, 124–131. [CrossRef]
85. Lemcke, K. Vertikalbewegungen des vormesozoischen Sockels im nördlichen Alpen-vorland Perm bis zur Gegenwart? *Eclogae Geol. Helv.* **1974**, *67*, 121–133.
86. Hetényi, G.; Plomerová, J.; Bianchi, I.; Kampfová Exnerová, H.; Bokelmann, G.; Handy, M.R.; Babuška, V. From mountain summits to roots: Crustal structure of the Eastenr Alps and Bohemian Massif along longitude 13.3 E. *Tectonophysics* **2018**, *744*, 239–255. [CrossRef]
87. Rosenberg, C.L.; Berger, A. On the causes and modes of exhumation and lateral growth of the Alps. *Tectonics* **2009**, *28*, TC6001. [CrossRef]
88. Kempf, O.; Pfiffner, O.A. Early Tertiary evolution of the North Alpine Foreland Basin of the Swiss Alps and adjoining areas. *Basin Res.* **2004**, *16*, 549–567. [CrossRef]
89. Schlunegger, F.; Burbank, D.W.; Matter, A.; Engesser, B.; Mödden, C. Magnetostratigraphic calibration of the Oligocene to Middle Miocene (30–15 Ma) mammal biozones and depositional sequences of the Swiss Molasse Basin. *Eclogae Geol. Helv.* **1996**, *89*, 753–788.
90. Van der Boon, A.; Beniest, A.; Ciurej, A.; Gaździcka, E.; Grothe, A.; Sachsenhofer, R.F.; Langereis, C.G.; Krijgsman, W. The Eocene-Oligocene trnasition in the North Alpine Foreland Basin and subsequent closure of a Paratethys gateway. *Glob. Planet. Chang.* **2018**, *162*, 101–119. [CrossRef]
91. Engesser, B. New Eomyidae, Dipodidae, and Cricetidae (Rodentia, Mammalia) of the Lower Freshwater Molasse of Switzeraland and Savoy. *Eclogae Geol. Helv.* **1987**, *80*, 943–994.
92. Diem, B. Die Untere Meeresmolasse zwischen der Saane (Westschweiz) und der Ammer (Oberbayern). *Eclogae Geol. Helv.* **1986**, *79*, 493–559.
93. Sachsenhofer, F.; Leitner, B.; Linzer, H.-G.; Bechtel, A.; Ćorić, S.; Gratzer, R.; Reischenbacher, D.; Soliman, A. Deposition, erosion and hydrocarbon source potential of the Oligocene Eggerding Formation (Molasse basin, Austria). *Austrian J. Earth Sci.* **2010**, *103*, 76–99.
94. Bernhardt, A.; Stright, L.; Lowe, D.R. Channelized debris-flow deposits and their impact on turbidity currents: The Puchkirchen axial channel belt in the Austrian Molasse Basin. *Sedimentology* **2012**, *59*, 2042–2070. [CrossRef]
95. Grunert, P.; Hinsch, R.; Sachsenhofer, R.F.; Bechtel, A.; Ćorić, S.; Harzhauser, M.; Piller, W.E.; Sperl, H. Early Burdigalian infill of the Puchkirchen Trough (North Alpine Foreland Basin, Central Paratethys): Facies development and sequence stratigraphy. *Mar. Pet. Geol.* **2013**, *39*, 164–186. [CrossRef]

96. De Ruig, M.J.; Hubbard, S.M. Seismic facies and reservoir characteristics of a deep-marine channel belt in the Molasse foreland basin. Puchkirchen Formation, Austria. *AAPG Bull.* **2006**, *90*, 735–752. [CrossRef]
97. Rubatto, D.; Regis, D.; Hermann, J.; Boston, K.; Engi, M.; Beltrando, M.; McAlpine, S.R. Yo-yo subduction recorded by accessory minerals in the Italian Western Alps. *Nat. Geosci.* **2011**, *4*, 338–342. [CrossRef]
98. Davis, J.H.; von Blanckenburg, F. Slab breakoff: A model of lithospheric detachment and its test in the magmatism and deformation of collisional orogens. *Earth Planet. Sci. Lett.* **1994**, *129*, 85–102. [CrossRef]
99. Schmid, S.; Aebli, H.R.; Heller, F.; Zingg, A. The role of the Periadriatic Line in the tectonic evolution of the Alps. In *Alpine Tectonics*; Coward, M.P., Dietrich, D., Park, R.G., Eds.; Geological Society: London, UK, 1989; Volume 45, pp. 153–171.
100. Engi, M.; Todd, C.S.; Schmalz, D.R. Tertiary metamorphic conditions in the eastern Lepontine Alps. *Schweiz. Mineral. Petrogr. Mitt.* **1995**, *75*, 347–369.
101. Boston, K.R.; Rubatto, J.; Hermann, J.; Engi, M.; Amelin, Y. Geochronology of accessory allanite and monazite in the Barrovian metamorphic sequence of the Central Alps, Switzerland. *Lithos* **2017**, *286*, 502–518. [CrossRef]
102. Kováč, M.; Nagymarosy, A.; Oszcypko, N.; Csontos, L.; Slaczka, A.; Marunteanu, M.; Matenko, L.; Márton, E. Palinspastic reconstruction of the Carpathian–Pannonian region during the Miocene. In *Geodynamic Development of the Western Carpathians*; Rakuš, M., Ed.; GUDS Bratislava: Bratislava, Slovakia, 1998; pp. 198–217.
103. Oszczypko, N. The structural position and tectonosedimentary evolution of the Polish Outer Carpathians. *Przegląd Geol.* **2004**, *52*, 780–791.
104. Bolliger, T.; Engesser, B.; Weidmann, M. Premiere Decouverte De Mammiferes Pliocenes Dans Le Jura Neuchateois. *Eclogae Geol. Helv.* **1993**, *86*, 1031–1068.
105. Sinclair, H.D. Flysch to Molasse transition in peripheral foreland basins: The role of the passive margin versus slab breakoff. *Geology* **1997**, *25*, 1123–1126. [CrossRef]
106. Lu, G.; Winkler, W.; Rahn, M.; von Quadt, A.; Willett, S.D. Evaluating igneous sources of the Taveyannaz formation in the Central Alps by detrital zircon U–Pb age dating and geochemistry. *Swiss J. Geosci.* **2018**, *111*, 399–416. [CrossRef]
107. Peresson, H.; Decker, K. Far-field effects of Late Miocene subduction in the Eastern Carpathians: E-W compression and inversion of structures in the Alpine-Carpathian-Pannonian region. *Tectonics* **1997**, *16*, 38–56. [CrossRef]
108. Frisch, W.; Kuhlemann, J.; Dunkl, I.; Skékely, B. The Dachstein paleosurface and the Augenstein Formation in the Northern Calcareous Alps–A mosaic stone in the geomorphological evolution of the Eastern Alps. *Int. J. Earth Sci.* **2001**, *90*, 500–518. [CrossRef]
109. Berger, J.-P. Paléontologie de la Molasse de Suisse Occidentale, taxonomie, biostratigraphie, paléoecologie et paléoclima tologie. Habilitation Thesis, University Fribourg, Fribourg, Switzerland, 1992; p. 405.
110. Ford, M.; Lickorish, H. Forleand basin evolution around the western Alpine arc. In *Deep-Water Sedimentation in the Alpine Basin of SE France*; New Perspectives on the Grès d'Annot and Related Systems; Joseph, P., Lomas, S.A., Eds.; Geological Society of London: London, UK, 2004; Volume 221, pp. 39–63.
111. Charollais, J.; Weidmann, M.; Berger, J.-P.; Engesser, B.; Hotellier, J.-F.; Gorin, G.; Reichenbacher, B.; Schäfer, P. La Molasse du bassin franco-genevois et son substratum. *Arch. Sci.* **2007**, *60*, 59–174.
112. Garefalakis, P.; Schlunegger, F. Tectonic processes, variations in sediment flux, and eustatic sea level recorded by teh 20 Myr old Burdigalian transgression in the Swiss Molasse basin. *Solid Earth* **2019**, *10*, 2045–2072. [CrossRef]
113. Keller, B. Fazies und Stratigraphie der Oberen Meeresmolasse (Unteres Miozän) Zwischen Napf und Bodensee. Ph.D. Thesis, University of Bern, Bern, Switzerland, 1989; p. 302.
114. Schlunegger, F.; Jordan, T.E.; Klaper, E.M. Controls of erosional denudation in the orogen on foreland basin evolution: The Oligocene central Swiss Molasse Basin as an example. *Tectonics* **1997**, *16*, 823–840. [CrossRef]
115. Krsnik, E.; Methner, K.; Campani, M.; Botsyun, S.; Mutz, S.G.; Ehlers, T.A.; Kempf, O.; Fiebig, J.; Schlunegger, F.; Mulch, A. Miocene high elevation in the Central Alps. *Solid Earth* **2021**, *12*, 2615–2631. [CrossRef]
116. Bernhard, R.; Sinclari, H.D.; Gailleton, B.; Fox, M. Formation of Longitudinal River Valleys and the Fixing of Drainage Divides in Response to Exhumation of Crystalline Basement. *Geophys. Res. Lett.* **2021**, *48*, e2020GL092201. [CrossRef]
117. Kühni, A.; Pfiffner, O.A. Drainage patterns and tectonic forcing: A model study for the Swiss Alps. *Basin Res.* **2001**, *13*, 169–197. [CrossRef]
118. Schlunegger, F.; Melzer, J.; Tucker, G. Climate, exposed source-rock lithologies, crustal uplift and surface erosion: A theoretical analysis calibrated with data from the Alps/North Alpine foreland basin system. *Int. J. Earth Sci.* **2001**, *90*, 484–499. [CrossRef]
119. Schlunegger, F.; Willett, S.D. Spatial and temporal variations in exhumation of the central Swiss Alps and implications for exhumation mechanisms. In *Exhumation Processes: Normal Faulting, Ductile Flow and Erosion*; Ring, U., Brandon, M.T., Lister, G.S., Willett, S.D., Eds.; Geological Society of London: London, UK, 1999; Volume 154, pp. 157–179.
120. Girault, J.-P.; Bellahsen, N.; Bernet, M.; Pik, R.; Loget, N.; Lasseur, E.; Rosenberg, C.L.; Balvay, M.; Sonnet, M. Exkumation of the Western Alpine collisional wedge: New thermochronological data. *Tectonophysics* **2021**, *822*, 229155. [CrossRef]
121. Girault, J.B. *Exhumation du Prisme Collisionnel Ouest Alpin et Évolution Girault, J.B. Exhumation du Prisme Collisionnel Ouest Alpin et Évolution du Bassin Molassique: Nouvelles Données Thermochronologiques et Tectono-Sédimentaires. Sciences de la Terre*; Sorbonne Université: Paris, France, 2020; NNT: 2020SORUS086. tel-03372619.
122. Allen, P.A.; Bass, J.P. Sedimentology of the Upper Marine Molasse of the Rhône-Alp region, Eastern France: Implications for basin evolution. *Eclogae Geol. Helv.* **1993**, *86*, 121–171.

123. Kalifi, A.; Sorrel, P.; Leloup, P.-H.; Galy, A.; Spina, V.; Huet, B.; Russo, S.; Pittet, B.; Rubino, J.-L. Tectonic control on the paleogeographical evolution of the Miocene Seaway along the Western Alpine foreland basin. In *Straits and Seaways: Controls, Processes and Implications in Modern and Ancient Systems*; Rossi, V.M., Longhitano, S., Olariu, C., Chiocci, F., Eds.; Geological Society of London: London, UK, 2022; Volume 523, *in press*. [CrossRef]
124. Bellahsen, N.; Mouthereau, F.; Boutoux, A.; Bellanger, M.; Lacombe, O.; Jolivet, L.; Rolland, Y. Collision kinematics in the western external Alps. *Tectonics* **2014**, *33*, 1055–1088. [CrossRef]
125. Herwegh, M.; Berger, A.; Baumberger, R.; Wehrens, P.; Kissling, E. Large-scale crustal-block-extrusion during late Alpine collision. *Sci. Rep.* **2017**, *7*, 413. [CrossRef]
126. Allen, P.A.; Mange-Rajetky, A.; Matter, A. Dynamic palaeogeography of the open Burdigalian seaway, Swiss Molasse basin. *Eclogae Geol. Helv.* **1985**, *78*, 351–381.
127. Martel, A.T.; Allen, P.A.; Slingerland, R. Use of tidal-circulation modeling in paleogeographical studies: An example from the Tertiary of the Alpine perimeter. *Geology* **1994**, *22*, 925–928. [CrossRef]
128. Dal Zilio, L.; Kissling, E.; Gerya, T.; van Dinther, Y. Slab rollback orogeny model: A test of concept. *Geophys. Res. Lett.* **2020**, *47*, e2020GL089917. [CrossRef]
129. Willett, S.D.; Schlunegger, F.; Picotti, V. Messinian climate change and erosional destruction of the central European Alps. *Geology* **2006**, *34*, 613–616. [CrossRef]
130. Kuhlemann, J. Postcollisional sediment budget of circum-Alpine basins (central Europe). *Mem. Sci. Geol. Univ. Padova* **2000**, *52*, 1–91.
131. Kuhlemann, J.; Frisch, W.; Dunkl, I.; Skékely, B. Quantifying tectonic versus erosive denudation by the sediment budget: The Miocene core complexes of the Alps. *Tectonophysics* **2001**, *330*, 1–23. [CrossRef]
132. Ji, W.-Q.; Malusà, M.G.; Tiepolo, M.; Langone, A.; Zhao, L.; Wu, F.-Y. Synchronous Periadriatic magmatism in the Western and Central Alps in the absence of slab breakoff. *Terra Nova* **2019**, *31*, 120–128. [CrossRef]
133. Mellere, D.; Stefani, C.; Angevine, C. Polyphase tectonics through subsidence analysis: The Oligo-Miocene Venetian and Friuli Basin, north-east Italy. *Basin Res.* **2020**, *12*, 159–182. [CrossRef]
134. Jost, J.; Kempf, O.; Kälin, D. Stratigraphy and palaeoecology of the Upper Marine Molasse (OMM) of the central Swiss Plateau. *Swiss J. Geosci.* **2016**, *109*, 149–169. [CrossRef]